*Review*

# Advances in Photothermal Therapy for Oral Cancer

Jian Liang [1,2,3,†], Pei Wang [1,2,3,†], Yanfang Lin [1,2,3], Ao Jia [1,2,3], Fei Tong [1,2,3,*] and Zhihua Li [1,2,3,*]

1  School of Stomatology, Jiangxi Medical College, Nanchang University, Nanchang 330006, China;
   liangjian673@email.ncu.edu.cn (J.L.); ndfskqyy620@ncu.edu.cn (P.W.); 413009220003@email.ncu.edu.cn (Y.L.);
   ndfskqyy667@ncu.edu.cn (A.J.)
2  Jiangxi Provincial Key Laboratory of Oral Diseases, Nanchang 330006, China
3  Jiangxi Provincial Clinical Research Center for Oral Diseases, Nanchang 330006, China
*  Correspondence: ndfskqyy315@ncu.edu.cn (F.T.); ndfskqyy140@ncu.edu.cn (Z.L.)
†  These authors contributed equally to this work.

**Abstract:** Oral cancer represents a critical global health issue, where traditional treatment modalities are often characterized by considerable adverse effects and suboptimal effectiveness. Photothermal therapy (PTT) offers an innovative method for tumor treatment, leveraging photothermal agents to convert light into hyperthermia, ultimately leading to tumor ablation. PTT offers unique advantages in treating oral cancer due to its superficial anatomical location and consequent accessibility to laser irradiation. PTT's advantage is further enhanced by its capacity to facilitate drug release and promote tissue regeneration. Consequently, the application of PTT for oral cancer has garnered widespread interest and has undergone rapid development. This review outlines advances in PTT for oral cancer, emphasizing strategies to improve efficacy and combination therapy approaches. The key challenges, including temperature control and long-term biosafety, are discussed alongside future directions. The review also encompasses PTT's role in managing oral potentially malignant disorders and postoperative defects, conditions intimately linked with oral cancer. We aim to provide guidance for emerging PTT research in oral cancer and to promote the development of precise and efficient treatment strategies.

**Keywords:** photothermal therapy; oral cancer; oral squamous cell carcinoma; oral potentially malignant disorders; nanomaterials

## 1. Introduction

Oral cancer, a malignancy predominantly arising in the lip mucosa, gingiva, tongue dorsum, palate, buccal mucosa, and floor of the mouth, poses a significant global health threat, severely compromising quality of life and survival [1–4]. According to global cancer statistics, approximately 380,000 new diagnoses and 180,000 deaths occur annually, constituting 2% of global cancer-related mortality [5–7]. Primary risk factors encompass tobacco use, betel quid chewing, alcohol consumption, and mechanical irritation such as residual roots [8–12]. Notably, oral potentially malignant disorders (OPMDs), like leukoplakia and erythroplakia, exhibit morphological alterations that confer an increased risk of malignant transformation over normal mucosa and consequently warrant significant attention [13–16]. The predominant type of oral cancer, oral squamous cell carcinoma (OSCC), accounts for more than 90% of cases, and most patients present with advanced disease [17–19]. Frequent local invasion and regional lymph node metastasis underscore the critical need for early diagnosis and intervention [20–24].

The oral and maxillofacial region, essential for speech, mastication, respiration, and aesthetics, presents a therapeutic dilemma: balancing radical tumor eradication with functional

preservation [25–27]. Current clinical paradigms rely on surgery, supplemented by adjuvant radiotherapy or chemotherapy [28,29]. However, these approaches face limitations: (1) surgical disfigurement and functional impairment [30]; (2) radiotherapy-induced complications (e.g., oral mucositis, xerostomia, osteoradionecrosis) [31]; and (3) chemotherapy-related systemic toxicity, myelosuppression, and multidrug resistance [32,33]. Consequently, despite significant advances in therapeutic procedures over recent decades, the 5-year survival rate remains consistently around 60%, and roughly one-third of treated patients experience relapse [34]. Furthermore, postoperative quality of life is greatly compromised, with studies indicating that 73.9% report dysphagia [35,36]. These challenges have spurred the development of novel strategies, including immunotherapy [37], molecular targeting [38], photodynamic therapy (PDT) [39], and photothermal therapy (PTT) [40].

PTT, an emerging modality, leverages photothermal agents (PTAs) to convert near-infrared (NIR) light into localized hyperthermia, selectively ablating heat-sensitive cancer cells while sparing healthy tissues [41,42]. Its advantages include non-invasiveness, spatiotemporal precision, repeatability, and synergistic potential with other therapies [43–45]. Beyond direct tumor ablation, PTT-generated heat enhances drug delivery, stimulates immunogenic antigen release, remodels the tumor microenvironment (TME), and promotes osteogenesis and soft tissue regeneration—critical for repairing post-resection maxillofacial defects [46–49]. Two factors dictate PTT efficacy: PTAs and light sources [50]. While NIR-II lasers (1000–1700 nm) address penetration depth limitations in superficial oral cancers, suboptimal PTAs performance—low photothermal conversion efficiency (PCE) and poor tumor targeting—remains a hurdle [51,52]. Recent advances in nanotechnology have yielded innovative nanomedical platforms to enhance PTAs accumulation (e.g., ligand-mediated targeting, stimuli-responsive release) and enable image-guided precision [53–55]. Furthermore, mild hyperthermia (40–45 °C) has been shown to stimulate osteoprogenitor proliferation and angiogenesis, facilitating post-surgical bone and soft tissue regeneration [56–58].

This review comprehensively explores four dimensions of PTT in oral oncology: (1) strategies to enhance PTAs' performance; (2) synergistic PTT-based combinatorial therapies; (3) multifunctional PTT systems integrating tumor ablation and tissue repair; and (4) PTT applications in OPMDs management (Figure 1). We highlight cutting-edge nano platform designs, targeted delivery mechanisms, and clinical translation challenges (such as long-term biosafety and temperature control) (Table 1). By bridging preclinical innovation and clinical needs, this work aims to catalyze the development of precision-engineered, multifunctional PTT strategies to improve therapeutic outcomes and enhance the overall patient survival rate in oral cancer.

**Table 1.** Summaries of photothermal therapy (PTT) for oral cancer and oral potentially malignant disorders (OPMDs).

| Disease Type | Therapy Mode | Photothermal Agents | Functionalization | Exposure Conditions | Tumor Type | Therapeutic Highlights | Ref. |
|---|---|---|---|---|---|---|---|
| Oral Cancer | PTT | AuNRs | PEG conjugated | 808 nm, 5.8 W cm$^{-2}$ | HSC 3 cells | 28 × 8 nm AuNRs are a more effective photothermal contrast agent for PTT of OSCC | [59] |
| | | | Thiolated PEG conjugated | 808 nm, 0.9–1.9 W cm$^{-2}$ | HSC 3 cells, CDX mouse model | Preferential tumor accumulation of Pegylated AuNRs indicates the selectivity and specificity of PTT | [60] |
| | | | Folate conjugated | 755 nm, 40 J cm$^{-2}$ | KB cells | Folic acid for active tumor targeting | [61] |

**Table 1.** *Cont.*

| Disease Type | Therapy Mode | Photothermal Agents | Functionalization | Exposure Conditions | Tumor Type | Therapeutic Highlights | Ref. |
|---|---|---|---|---|---|---|---|
| | | | Cysteine-functionalized alginate and cyclic peptide, c(RGDfK)KKK modified | 808 nm, 2 W cm$^{-2}$ | SAS 3 cells, CDX mouse models | Replacing cetyltrimethy-lammonium bromide (CTAB) with alginate improves the biocompatibility of AuNRs | [62] |
| | | | PLTs loaded | 808 nm, 2 W cm$^{-2}$ | CAL 27 cells, CDX mouse model, HNSCC-bearing *Tgfbr1/Pten* 2cKO mouse model | PTT enhances tumor targeting of PLT-AuNRs, which in turn improves PTT effects via a feedback mechanism, demonstrating the benefit of PLT-PTT in cancer therapy | [63] |
| | | | Anti-EGFR antibodies conjugated | 800 nm, 10–20 W cm$^{-2}$ | HOC 313 cells, HSC 3 cells | Integrated molecular imaging with photothermal cancer therapy | [64] |
| | | AuNPs | — | 532 nm, 0.3 W cm$^{-2}$ | DMBA-induced HBP carcinoma | Plasmonic photothermal therapy on induced HBP carcinoma | [65] |
| | | | Anti-EGFR antibodies conjugated | 514 nm, 13–64 W cm$^{-2}$ | HSC 313 cells, HOC 3 cells | Selective PTT for epithelial carcinoma | [66] |
| | | CuS NPs | BSA-templated synthesis of BSA@CuS nanoparticles with subsequent PEGylation | 1064 nm, 0.5 W cm$^{-2}$ | CAL 27 cells, SCC 9 cells, CDX mouse model | Modified with PEG to increase biocompatibility | [67] |
| | | Ag$_3$AuS$_2$ NPs | Ag$_3$AuS$_2$ NPs complexed with genetically engineered anionic protein and chitosan | 808 nm, 1 W cm$^{-2}$ | CAL 27 cells, CDX mouse model | Features tongue tumor inhibition and complication prevention | [68] |
| | | Gold-silica nanoshells | Anti-HER2 nanobodies conjugated | 820 nm, 4 W cm$^{-2}$ | KB cells | First in vitro investigation of PTT efficacy using anti-HER2 nanobody-conjugated nanoshells in an OSCC model | [69] |
| | | Fe$_3$O$_4$ NPs | Platelet-cancer stem cell hybrid membrane coated | 808 nm, 5 W cm$^{-2}$ | CAL 27 cells, CDX mouse model, HNSCC-bearing *Tgfbr1/Pten* 2cKO mouse model | First presentation of a platelet–cancer stem cell hybrid membrane-coated iron oxide magnetic nanoparticle for enhanced PTT of HNSCC | [70] |
| | | Au@C NPs | Membrane of patient-derived cells coated | 808 nm, 1 W cm$^{-2}$ | CAL 27 cells, SCC 7 cells, HN 6 cells, CDX mouse model, orthotopic tongue tumor mouse model, primary and distant tumor mouse models, PDX mouse model | The homologous cancer cell membrane provided the nanoplatforms with optimal targeting properties for maximum therapeutic efficiency | [71] |
| | | BP NSs | PDA and polyacrylamide hydrochloride-dimethylmaleic acid (PAH-DMMA) charge reversal system modified | 808 nm, 1.5 W cm$^{-2}$ | CAL 27 cells, SAS cells, CDX mouse model | Nanoplatforms exhibit suitable size for intravenous delivery, enrichment in tumor sites, enhanced tumor cell uptake, excellent photothermal properties, and effective oral cancer cell killing | [72] |
| | | Carbon dots | Triton-X-directed synthesis of N-rich mesoporous carbon nanospheres from pyrrole and aniline | 980 nm, 1.4 W cm$^{-2}$ | FaDu cells | Exhibiting integrated PTT and FL functionalities | [73] |

**Table 1.** *Cont.*

| Disease Type | Therapy Mode | Photothermal Agents | Functionalization | Exposure Conditions | Tumor Type | Therapeutic Highlights | Ref. |
|---|---|---|---|---|---|---|---|
| | | Semiconductor polymer (PCPDTBT) | Incorporated gadolinium-grafted triblock amphiphilic copolymer (F127-DTPA-Gd) | 808 nm, 1 W cm$^{-2}$ | SCC 7 cells, CDX mouse model | Two-component nanotheranostic platform enabling efficient MRI and FL-guided PTT | [74] |
| | | GO | Amino-modified | 808 nm, 2 W cm$^{-2}$ | HSC 3 cells, CDX mouse model | Graphene-based nanomaterials as direct nano-PTAs for anticancer PTT | [50] |
| | | Gold nanodots | Peptide HN-1 modified | 808 nm, 2 W cm$^{-2}$ | SCC 9 cells, CAL 27 cells, CRL 1623 cells, CDX mouse model | Versatile nanosystem for targeted drug delivery and diagnostic imaging | [54] |
| | | Au/Mn nanodots | — | 1064 nm, 2 W cm$^{-2}$ | SCC 9 cells, CAL 27 cells, CDX mouse model | Features multimodal bioimaging, including concurrent CT and MRI, and bright near-infrared FL for navigation | [75] |
| | | ICG | Functionalized with cypate fluorophore and two cyclic-(arginine-glycine-aspartic acid) (cRGD) peptides | 808 nm, 1 W cm$^{-2}$ | CAL 27 cells, CDX mouse model | ICG-derived NIR fluorescent probes designed and synthesized for accurate diagnosis and treatment | [76] |
| | | Aggregation-induced emission luminogens (AIEgen) | NMB@NPs constructed from carbon radical monomer, ethyl 2,6-diisocyanatohexanoate, PEG molecules, and an AIEgen | 808 nm, 1 W cm$^{-2}$ | CAL 27 cells, PDX mouse model | FL-guided thermodynamic therapy and PTT | [77] |
| | | MXene NSs | Incorporated into a scaffold created from collagen, silk, and hydroxyapatite | 808 nm, 1 W cm$^{-2}$ | CAL 27 cells, bone defect rabbit model | Simultaneously kills OSCC cells and promotes bone tissue regeneration | [56] |
| | | Ti$_3$C$_2$ Mxene | Scaffold constructed from Ti$_3$C$_2$ MXene, collagen, and silk fibroin | 808 nm, 1 W cm$^{-2}$ | SCC 25 cells, CAL 27 cells, CDX mouse model | Exhibits simultaneous OSCC cell cytotoxicity and mucosal defect regeneration | [57] |
| | | ICG | Scaffold fabricated with collagen/silk fibroin and ICG | 808 nm, 1 W cm$^{-2}$ | SCC 25 cells, CDX mouse model | Facilitated the attachment and proliferation of rat buccal mucosa fibroblasts and enhanced the repair of buccal mucosal wounds | [58] |
| | PTT, PDT | AuNRs | Rose bengal molecules conjugated | 810 nm, 17.86 W cm$^{-2}$, 532 nm, 1.76 W cm$^{-2}$ | CAL 27 cells, DMBA-induced HBP carcinoma | Combined PDT/PTT capabilities against oral cancer | [78] |
| | | Organic compound (C3) | ICG and C3 encapsulated within PEG-PCL | 808 nm, 0.5 W cm$^{-2}$ | HSC cells, CDX mouse model | FL-guided PTT/PDT against OSCC | [45] |
| | | Au nanoflower | Two layers of silica shell ICG added | 808 nm, 10 W cm$^{-2}$ | Cal 27 cells, CDX mouse model | Tumor growth inhibition through synchronous PTT and PDT | [79] |
| | | AuNPs | Sulfonated aluminum phthalocyanines conjugated | 1064 nm, 39.9–420.1 W cm$^{-2}$ | SAS cells | Effective inactivation of oral cancer cells via combined PTT and PDT effects | [80] |
| | | Au nanopopcorns | Stabilized with PEG through 11-mercaptoundecanoic acid and coated with silicon 2,3-naphthalocyanine dihydroxide | 808 nm, 0.55 W cm$^{-2}$ | KB-3-1 cells, SK-BR-3 cells | First application of magnetic-field-guided drug delivery and dual-mode PTT/PDT using magnetic-optical hybrid nanosystems | [81] |
| | | Cu$_{2-x}$S | Magnetic manganese compounds integrated | 808 nm, 0.72 W cm$^{-2}$ | HeLa cells, CDX mouse model, PDX mouse model | Reactive oxygen species (ROS) and heat generation enhance PTT, and O$_2$ self-supplementation enhances PDT | [82] |
| | | ICG, SWCNTs | ICG-conjugated hyaluronic acid nanoparticles encapsulated within SWCNTs | 808 nm, 0.8 W cm$^{-2}$ | SCC 7 cells, CDX mouse model | CD44-targeted theranostic nanoparticle for PA image-guided dual PTT and PDT cancer therapy | [83] |

Table 1. *Cont.*

| Disease Type | Therapy Mode | Photothermal Agents | Functionalization | Exposure Conditions | Tumor Type | Therapeutic Highlights | Ref. |
|---|---|---|---|---|---|---|---|
| | | Cobalt-glycerate nanosheets | Folic acid modified | 808 nm, 1.2 W cm$^{-2}$ | CAL 27 cells, residual OSCC tumors bearing mouse model, CDX mouse model | MRI-guided postsurgical PTT/PDT | [84] |
| | | Au, Ce6 | Polyethyleneimine functionalized with Au and Pt, followed by attachment of Ce6 and HN-1 | 1064 nm, 2 W cm$^{-2}$, 650 nm, 0.5 W cm$^{-2}$ | SCC 9 cells, CDX mouse model | CT/FL/photothermal tri-modal imaging-guided treatment | [85] |
| | PTT, chemotherapy | ICG | Nanoparticles co-assembled from hydrophilic linear PEG and hydrophobic cholic acid cluster amphiphilic subunits | 808 nm, 0.8 W cm$^{-2}$ | OSC 3 cells, orthotopic CDX mouse model, metastatic CDX mouse model | Versatile chemo-nanoplatform for synergistic PTT/chemotherapy of orthotopic oral cancer and immuno-nanoplatform for synergistic PTT/immunotherapy of metastatic cancer | [86] |
| | | | DOX-encapsulated PLGA nanoparticles with a cancer cell membrane and ICG surface coating | 808 nm, 1.5 W cm$^{-2}$ | HSC 3 cells, CDX mouse model | Selective cancer cell targeting and induction of intrinsic mitochondria-mediated apoptosis via the p53 signaling pathway | [55] |
| | | IR820 | IR820/methylcellulose hydrogel containing mesoporous silica nanoparticles and DOX | 808 nm, 2 W cm$^{-2}$ | CAL 27 cells, CDX mouse model | Long-term synergistic antitumor activity with lower toxicity | [87] |
| | | | IR820 and curcumin loaded onto hyaluronic acid microneedles | 808 nm, 1 W cm$^{-2}$ | CAL 27 cells | Curcumin nanoparticles and IR820 microneedle combined drug delivery systems (DDS) have complete morphology and good mechanical properties | [88] |
| | | AuNRs | Silica-coated AuNRs with a covalently assembled amphiphilic PLGA-PEG polymeric corona loaded with vincristine | 808 nm, 1.2 W cm$^{-2}$ | SCC 15 cells, DMBA-induced HBP carcinoma | Coronabased drug delivery approach exhibited superior anticancer effects on OSCC | [89] |
| | | | Folate-targeted pegylated poly(D, L-lactide-co-glycolide) loaded with phytochemical anticancer thymoquinone and AuNRs | 808 nm, 1.2 W cm$^{-2}$ | SCC 15 cells, DMBA-induced HBP carcinoma | Strong synergistic anticancer effects and selective tumor targeting via a dual-modal approach | [90] |
| | | AuNPs | Endogenously double-controlled cisplatin prodrug incorporated | 808 nm, 0.3 W cm$^{-2}$ | 3D tumor models of SCC-25 and SCC-154 | The first multifunctional nano-architecture (tNAscisPt) for combined chemotherapy and PTT | [91] |
| | | | PEG-stabilized and conjugated with PDPN antibody and DOX | 532 nm, 1 W cm$^{-2}$ | CAL 27 cells, CDX mouse model | Versatile drug-delivery nanoplatforms for targeted and combined chemo-PTT against oral cancer | [92] |
| | | GO | PEGylated GO linked with DOX and FAP-targeted peptide chains | 808 nm, 1 W cm$^{-2}$ | CAL 27 cells, CDX mouse model | Precise targeting capability coupled with combined chemotherapy and PTT | [93] |
| | | | Modified with hyaluronic acid and HN-1 peptide and loaded with DOX | 808 nm, 1 W cm$^{-2}$ | CAL 27 cells, CDX mouse model | Effective targeting of OSCC cells and outstanding localized deposition in xenograft tumors | [94] |
| | | | Loaded with ATP citrate lyase specific inhibitor (SB-204990) and DOX | 808 nm, 1.5 W cm$^{-2}$ | SCC 15 cells, CDX mouse model | Synergistic treatment via lipid starvation, chemotherapy, and PTT | [95] |

<p align="center">**Table 1.** *Cont.*</p>

| Disease Type | Therapy Mode | Photothermal Agents | Functionalization | Exposure Conditions | Tumor Type | Therapeutic Highlights | Ref. |
|---|---|---|---|---|---|---|---|
| | | | GO and Cisplatin blended with poly(L-lactide) and hydroxypropyl methylcellulose | 808 nm, 1.5 W cm$^{-2}$ | Human oral squamous cell carcinoma cell line UPCI-SCC-084, cisplatin-resistant cell line, 3D tumor spheroid model | 3D-printed biodegradable implant with chemo-thermal ablation potential | [96] |
| | | Cu (II) | Enveloped by chitosan | 808 nm, 0.33 W cm$^{-2}$ | KB cells, CDX mouse model | Combined PTT and chemotherapy using CuCC NPs for noninvasive tumor ablation and reduced postoperative recurrence risk | [97] |
| | | | Polyethylene glycol-coated polyaniline NSs codoped with Cu (II) and vincristine | 808 nm, 0.33 W cm$^{-2}$ | KBV cells, KB cells, CDX mouse model | MDR-tumor-targeted theranostics utilizing strong electrostatic interactions between resistant cells and nanomaterials | [98] |
| | | Au nanoflowers | Two layers of silica coated | 808 nm, 5–9 W cm$^{-2}$ | CAL 27 cells, HepG2 cells | Potentials for versatile loading and delivery of chemotherapeutic or photodynamic drugs | [99] |
| | | Hollow mesoporous Prussian blue NPs (HMPBs) | DOX-loaded HMPBs within a hyaluronic acid microneedle system | 808 nm, 2 W cm$^{-2}$ | CAL 27 cells, CDX mouse model | Thermal ablation and DOX release, promoted by the generated heat, induced apoptosis of tumor cells | [100] |
| | | Chiral molybdenum (Cys-MoO$_{3-x}$) NPs | Decorated with cysteine molecules | 405–808 nm, 1 W cm$^{-2}$ | OSCC cells | Visible light and NIR dual-responsive properties for cancer cell ablation | [101] |
| | | PDA | Functionalized with S-nitrosothiol, surrounded by gambogic acid-conjugated hyaluronic acid shells | 808 nm, 1 W cm$^{-2}$ | HN6 cells, CDX mouse model | Tumor-selective nanocomplex for low-temperature photothermal therapy and NO-enhanced chemotherapy | [102] |
| | PTT, radiotherapy | AuNPs | Folate conjugated. | 532 nm, 0.47 W cm$^{-2}$ | KB cells | Folate-conjugated gold nanoparticles induced cytotoxicity and cell apoptosis in KB cells | [103] |
| | PTT, gene therapy | AuNRs | Complexed with anionic-charged siRNA oligos | 810 nm, 3.3 W cm$^{-2}$ | CAL 27 cells, CDX mouse model | Overcomes thermoresistance to sensitize cancer cells to hyperthermia | [104] |
| | PTT, immunotherapy | ICG | Gelatin nanoparticles loaded with ICG and NSC74859 (signal transducer activator of transcription 3, STAT3 inhibitor) | 808 nm, 1 W cm$^{-2}$ | CAL 27 cells, CDX mouse model, HNSCC-bearing *Tgfbr1/Pten* 2cKO mouse model | Photothermal destruction of tumors combined with the STAT3 inhibitor elicited potent antitumor immunity for enhanced cancer therapy | [105] |
| | | Organic photovoltaic material (PBDB-T NPs) | — | 660 nm, 0.6 W cm$^{-2}$ | CAL 27 cells, CDX mouse model, immuno-competent and syngeneic mouse tumor model | Enhanced mPTT efficacy and active tumor-specific adaptive immune responses | [106] |
| | | Molybdenum diphosphide nanorods (MoP$_2$ NRs) | — | 808 nm, 0.5 W cm$^{-2}$ | CAL 27 cells, SCC9 cells, CDX mouse model | Therapeutic modality via laser-potentiated peroxidase catalytic/mPTT | [107] |
| | | Fe$_3$O$_4$ NPs | — | 808 nm, 1 W cm$^{-2}$ | SCC 7 cells, CDX mouse model | Regulates the polarization of tumor-associated macrophages and enhances the inhibitory effect on tumor cells | [108] |

**Table 1.** *Cont.*

| Disease Type | Therapy Mode | Photothermal Agents | Functionalization | Exposure Conditions | Tumor Type | Therapeutic Highlights | Ref. |
|---|---|---|---|---|---|---|---|
| | | IR820 | TAT peptide-conjugated IR820 incorporated into Poly(N-isopropylacrylamide) (PNI-PAM)/demethylated lignin (DL) hydrogel | 808 nm, 2 W cm$^{-2}$ | SCC 7 cells, bacteria-colonized tumor spheroids, bacteria-colonized tumor-bearing mouse, lung metastasis model with bacterial colonization | Photothermal ablation with robust stimulation of antitumor immune responses against bacteria-colonized OSCC | [109] |
| | | AuNPs | Combined with cisplatin-loaded BP NSs | 808 nm | SCC 9 cells, DMBA-induced HBP carcinoma | High drug-loading capacity and excellent photothermal properties | [110] |
| | PTT, PDT, chemotherapy | ICG | Coordination compound of ICG-cisplatin encapsulated into human serum albumin | 808 nm, 2 W cm$^{-2}$ | HSC cells, CDX mouse model | Synergistic PTT/PDT/chemotherapy against OSCC via a NIR stimuli-responsive, tumor-targeted drug release system | [111] |
| | | Coi8DFIC-sorafenib NPs | Coi8DFIC dye and sorafenib were used to construct CS NPs | 808 nm, 0.5 W cm$^{-2}$ | CAL 27 cells, CDX mouse model | Laser on/off controlled vascular targeting therapy with CS NPs, guided by tumor-associated vessel tracking and real-time tumor imaging | [112] |
| | | Pheophorbidea, Pa | Pa and DOX self-assembled, followed by the introduction of dual-aldehyde terminated polyethylene glycol2000 (PEG-2CHO) | 680 nm, 0.4 W cm$^{-2}$ | OSC 3 cells, subcutaneous and orthotopic CDX tumor model | Dual size/charge-transformable Trojan-Horse nanoparticle for delivery of ultrasmall, full active pharmaceutical ingredients | [113] |
| | PTT, PDT, gene therapy | ICG | Poly($\beta$-amino ester)/PLGA blended nanoparticles loaded with ICG, surface-adsorbed with Nrf2-siRNA, and encapsulated within cancer cell membrane vesicles | 808 nm, 2 W cm$^{-2}$ | SCC 25 cells, CDX mouse model | Excellent PTT/PDT agent for OSCC treatment, where Nrf2-siRNA serves as an efficient photosensitizer synergist for PDT amplification | [114] |
| | | Ce6 | Simvastatin (SIM)-packaged Ce6-PEG with a surface modification of targeting-antibody (anti-low-density lipoprotein receptor) | 660 nm, 1 W cm$^{-2}$ | SCC 7 cells, homologous xenograft tumor mouse model | Cholesterol-regulating NPs with high tumor targeting and adjuvanticity for effective photo-induced immunotherapy | [115] |
| | PTT, PDT, immunotherapy | IR780 | Double-layered membrane vesicles extracted from attenuated *P. gingivalis* as an immune adjuvant | 808 nm, 1 W cm$^{-2}$ | SCC 7 cells, CDX mouse model, metastatic CDX mouse model | Double-layered membrane vesicles derived from *P. gingivalis* applied as a novel bacterial adjuvant for activating antitumor immunity | [116] |
| | | PDA | PDA-hyaluronic acid matrix loaded with protoporphyrin IX and aCD47-tagged CaCO$_3$ NPs | 808 nm, 1.2 W cm$^{-2}$, 660 nm, 0.04 W cm$^{-2}$ | CAL 33 cells, low-immunogenic OSCC mouse model, residual tumor mouse model, orthotopic and subcutaneous CDX mouse model | Effectively prevents local recurrence, inhibits orthotopic OSCC growth and pulmonary metastasis, and provides long-term protective immunity against tumor rechallenge | [117] |
| Oral leukoplakia (OLK) | PTT, PDT | ITIC-Th | — | 660 nm, 1 W cm$^{-2}$ | CAL 27 cells, 4-nitroquinoline 1-oxide (4NQO)-induce oral leukoplakia mouse model | Effectively suppresses OLK cancerization without apparent topical or systemic toxicity and represents the first interdisciplinary research in multimodal therapy for OLK | [118] |

**Table 1.** *Cont.*

| Disease Type | Therapy Mode | Photothermal Agents | Functionalization | Exposure Conditions | Tumor Type | Therapeutic Highlights | Ref. |
|---|---|---|---|---|---|---|---|
| | PTT, drug therapy | GO | Surface modification of GO with PEG via amide reaction, serving as a carrier to adsorb FAP targeting peptides and cyclooxygenase-2 inhibitors | 808 nm, 1 W cm$^{-2}$ | DOK cells, 4-nitroquinoline 1-oxide (4NQO)-induced oral precancerous mice model | Nano-drug delivery system for targeting OLK with high FAP expression | [119] |
| | PTT, PDT, drug therapy | Mesoporous polydopamine nanoparticles | ICG and celecoxib co-loaded onto mesoporous polydopamine nanoparticles | 808 nm, 1.5 W cm$^{-2}$ | DOK cells, 4-nitroquinoline 1-oxide (4NQO)-induced oral precancerous mice model | Transmucosal delivery of soluble microneedle-mediated integrated phototherapy anti-inflammatory NPs for OLK | [120] |

Abbreviation. 3D: Three-dimensional; AuNPs: Gold nanoparticles; AuNRs: Gold nanorods; BP: Black Phosphorus; BSA: Bovine serum albumin; CDX: Cell line-derived xenograft; Ce6: Chlorin e6; CT: Computed tomography; DMBA: 7,12-Dimethylbenz[a]anthracene; DOX: Doxorubicin; EGFR: Epidermal growth factor receptor; FAP: Fibroblast activation protein; FL: Fluorescence; GO: Graphene oxide; HBP: Hamster buccal pouch; HN-SCC: Head and neck squamous cell carcinoma; ICG: Indocyanine green; KBV: Human oral epithelial carcinoma vincristine-resistant tumor; mPTT: Mild-temperature photothermal therapy; MRI: Magnetic resonance imaging; NIR: Near-infrared; NSs: Nanosheets; OLK: Oral leukoplakia; OSCC: Oral squamous cell carcinoma; PA: Photoacoustic; PDA: Polydopamine; PDT: Photodynamic therapy; PDX: Patient-derived xenograft; *P. gingivalis*: *Porphyromonas gingivalis*; PLGA: Poly(lactic-co-glycolic acid); PLTs: Platelets; PTAs: Photothermal agents; PTT: Photothermal therapy; SWCNTs: Single-walled carbon nanotubes.
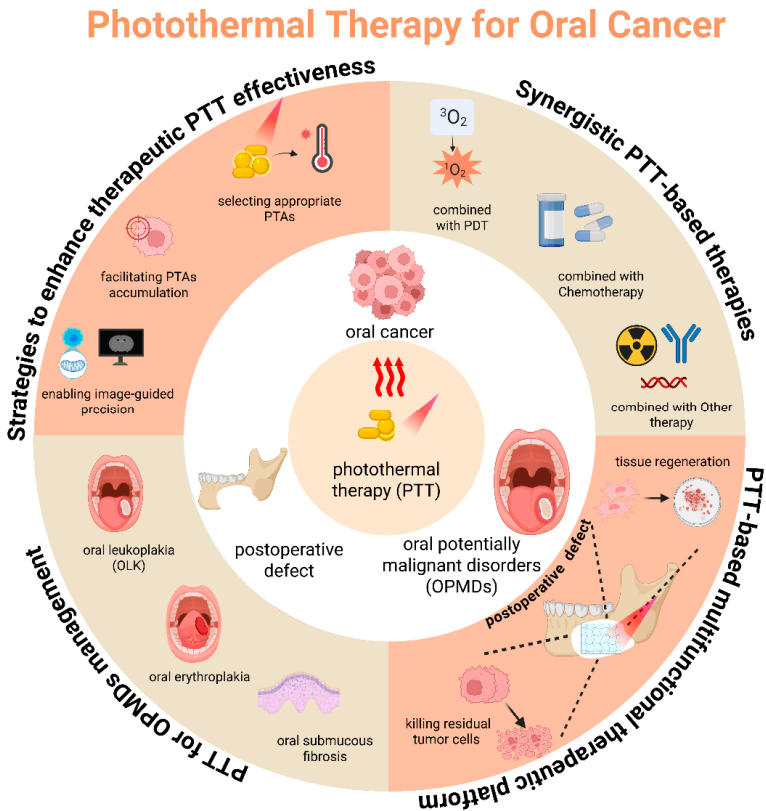


**Figure 1.** Schematic illustration of advances in photothermal therapy (PTT) for oral cancer. By leveraging photothermal agents (PTAs), PTT transforms near-infrared (NIR) light into localized hyperthermia, leading to the ablation of heat-sensitive oral cancer cells. Selecting appropriate PTAs, facilitating PTAs accumulation, and enabling image-guided precision to enhance the therapeutic effectiveness of PTT. Furthermore, when combined with other therapy modalities, PTT can exhibit synergistic effects against oral cancer. Beyond treatment, PTT can also be used for oral cancer prevention by inhibiting the malignant transformation of oral potentially malignant disorders (OPMDs) and for improving post-treatment quality of life by promoting tissue regeneration for postoperative tissue defects. Figure created using BioRender. Liang, J. (2025), https://BioRender.com/msdengq, accessed on 7 April 2025.

## 2. Strategies to Enhance PTT Therapeutic Effectiveness

The efficacy of PTT in treating oral cancer hinges on addressing three critical challenges: enhancing the PCE of PTAs, optimizing tumor-specific accumulation, and determining the optimal laser irradiation timing. Augmenting PCE of PTAs reduces the required agent concentration for tumor ablation, thereby minimizing long-term biotoxicity while concurrently lowering laser power and exposure duration to improve therapeutic safety and efficiency [121]. Enhancing tumor-targeted accumulation of PTAs mitigates off-target thermal damage to healthy tissues, a cornerstone strategy for amplifying PTT efficacy in oral oncology [122,123]. Furthermore, the dynamic biodistribution of PTAs necessitates precise temporal control, as irradiation during peak intratumoral accumulation maximizes ablation efficacy and minimizes collateral effects [124]. Real-time imaging-guided PTT, leveraging techniques such as photoacoustic tomography or fluorescence tracking, could synchronize laser activation with PTAs' pharmacokinetic peaks, enabling spatiotemporally precise therapy [125].

### 2.1. Selection of Appropriate PTAs

PTT hinges on PTAs to convert light energy into thermal energy, making PTAs the cornerstone of PTT efficacy. For optimal performance, PTAs should demonstrate a high PCE. Nanoparticles (NPs), owing to their strong NIR absorption capabilities, are widely utilized due to their superior PCE [126,127]. Nanomaterials employed in PTT for oral cancer can be categorized into four classes: noble metal nanomaterials, metal compounds, carbon-based nanomaterials, and organic nanoparticles [53]. Upon electromagnetic excitation, metallic nanoparticles exhibit localized surface plasmon resonance (LSPR), leading to intense electromagnetic energy absorption and subsequent heat generation through electron excitation and relaxation—a mechanism known as plasmonic photothermal therapy (PPTT), which demonstrates superior light absorption and thermal conversion efficiency compared to conventional PTT [128,129]. Coupled with inherent biocompatibility, these properties have driven the widespread adoption of metallic nanoparticles [130].

Among noble metal-based PTAs, gold nanomaterials (AuNPs) stand out as the most extensively studied due to their exceptional photothermal performance, tunable size/morphology, and low toxicity [65]. The heat generation capacity of AuNPs under NIR irradiation depends on their absorption cross-section and efficiency, which are governed by particle geometry and dimensions. Gold nanorods (AuNRs), in particular, exhibit optimal NIR absorption cross-sections and unparalleled PCE among plasmonic AuNPs [64]. Their photothermal performance is further modulated by factors such as absorption-to-extinction ratio, near-field electric field intensity, and decay length of the electric field beyond the nanoparticle surface [131]. Size-dependent studies reveal that $28 \times 8$ nm AuNRs outperform $17 \times 5$ nm or $38 \times 11$ nm counterparts in photothermal ablation efficiency, as demonstrated by Mackey et al. [59], establishing them as a gold standard for cancer cell eradication.

### 2.2. Accumulation of PTAs in Tumor Tissue

The insufficient intratumoral accumulation of PTAs necessitates higher dosages, prolonged laser exposure, or increased laser power, raising risks of off-target tissue damage. Thus, targeted delivery and retention of PTAs within tumors are critical for safe and efficient phototherapy. A key advantage of nanomaterial-based cancer therapy lies in exploiting the tumor's unique vascular leakage [132]. Rapid angiogenesis within tumors leads to aberrant vasculature and compromised lymphatic drainage, collectively giving rise to the enhanced permeability and retention (EPR) effect—an inherent "passive targeting" mechanism within the tumor microenvironment [133]. However, despite leveraging EPR-driven passive tar-

geting, PTAs accumulation in tumors remains suboptimal, necessitating more efficient and active targeting strategies to enhance tumor-specific cellular uptake and minimize nonspecific biodistribution [61]. Active targeting exploits overexpressed cell surface markers (such as receptors) to selectively direct PTAs to cancer cells [134,135]. Nanoparticles possess a high surface-area-to-volume ratio, enabling dense surface functionalization with various targeting moieties, including antibodies, small molecules, peptides such as anti-epidermal growth factor receptor (anti-EGFR) [64], HN-1 peptide [54], SERPINH1 antibody [135], Arg–Gly–Asp (RGD) peptide [136]. Compared with PTT alone, active targeting enables malignant cell ablation at lower temperatures, requiring only half the energy needed to disrupt normal cells at equivalent nanorod-bioconjugate concentrations, thereby enhancing therapeutic specificity and reducing side effects [64]. Biomimetic nanoparticles coated with cell membranes derived from stem cells [70], cancer cell membranes [55,137], or platelets [63] have recently gained attention due to their superior biocompatibility and homologous targeting properties. For instance, Bu et al. [70] demonstrated that iron oxide magnetic nanoparticles coated with a platelet-cancer stem cell hybrid membrane ([CSC-P]MNs) resulted in greater tumor accumulation, less uptake by the spleen and liver, and diminished metabolic activity, thus enhancing PTT therapeutic efficacy (Figure 2A). These coatings prolong circulation time and enhance tumor accumulation through immune evasion and tissue-specific homing.
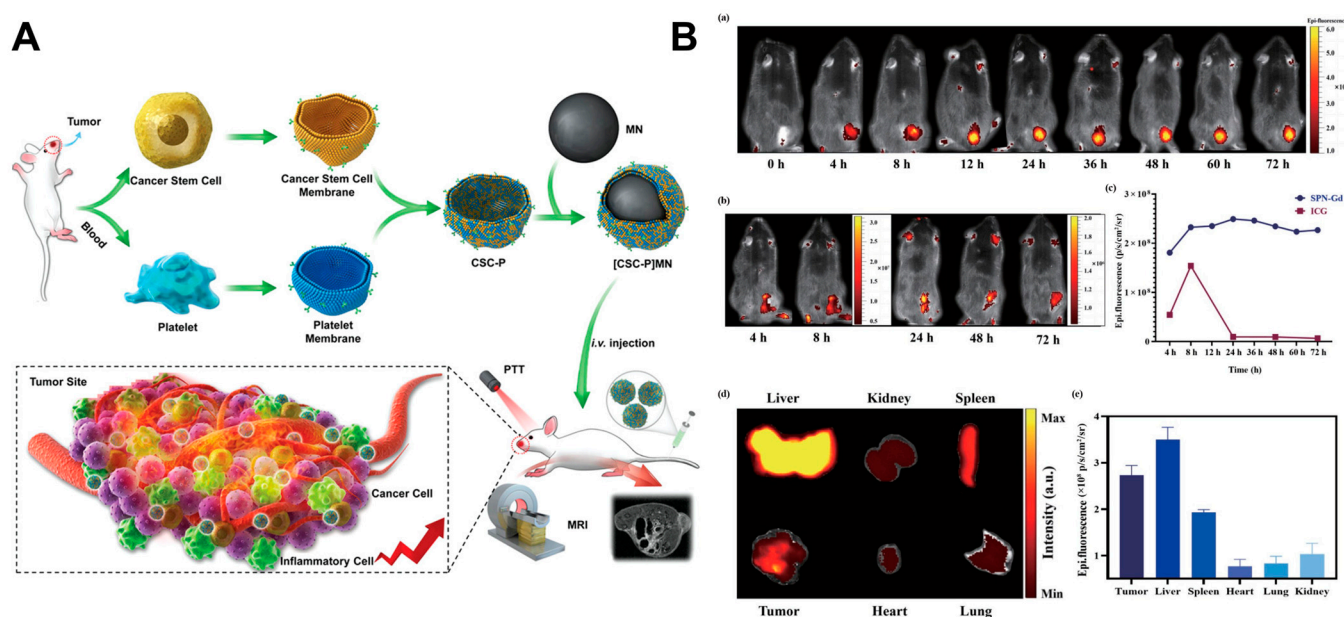


**Figure 2.** Strategies to enhance PTT therapeutic effectiveness. (**A**) Schematic illustration of [CSC-P]MNs and their application in cancer theranostics. Reproduced with permission [70]. Copyright 2019, John Wiley and Sons Group (Hoboken, NJ, USA). (**B**) (**a**) Fluorescence images at different time points following injection of SPN-Gd, (**b**) fluorescence images at different time points following indocyanine green injection, (**c**) comparison of fluorescence signal intensity between SPN-Gd and indocyanine green at different time points, (**d**,**e**) fluorescence signal intensity of main organs and tumors 72 h following injection of SPN-Gd. Reproduced with permission [74]. Copyright 2022, Springer Nature Group (Berlin, Germany).

Drug delivery systems (DDS) co-loaded with PTAs further optimize therapeutic outcomes. Nanoparticle-based DDS improves pharmacokinetics by enhancing drug stability, extending half-life, and preventing premature release [138]. Stimuli-responsive DDS, activated by tumor microenvironment cues (e.g., pH [95,96]) or external triggers (e.g., light [77,99]), enable spatiotemporally controlled drug release [139]. For instance, pH-responsive charge-

reversal nanodrug systems initially maintain a negative surface charge in circulation to minimize clearance [72,98]. Upon reaching acidic tumor regions, dimethylmaleamide cleavage converts the surface charge to positive, enhancing tumor penetration, cellular uptake, and localized drug release [72]. Coupled with intrinsic photothermal properties, such systems achieve synergistic tumor ablation and chemotherapy.

While intravenous administration dominates PTAs delivery, the superficial location of oral cancers enables alternative localized strategies [140,141]. Injectable hydrogels, administered via peritumoral or intratumoral routes, offer precise PTAs deposition. For example, E72-chitosan hydrogels injected around tongue tumors degrade within 24 h, ensuring prolonged local retention of inorganic NPs [68]. Single-session PTT with this approach achieves complete tumor eradication without functional compromise or systemic toxicity. Intratumoral injection further concentrates PTAs within lesions, maximizing hyperthermia efficacy. Post-PTT, residual PTAs are expelled alongside necrotic tissue, eliminating systemic absorption risks [50].

### 2.3. Navigation from Imaging

Systemic administration of PTAs in many studies results in their circulation through the vasculature and subsequent accumulation in tumors via the EPR effect. The pharmacokinetic properties of PTAs exhibit significant variability based on their physicochemical characteristics [124]. Optimal therapeutic outcomes are typically achieved when PTT is initiated at peak intratumoral PTAs accumulation. To address this, researchers have integrated imaging-guided strategies to monitor PTAs biodistribution in real-time, enabling laser irradiation at maximal tumor retention and dynamic adjustment of dosing regimens [84,85]. This approach minimizes off-target toxicity while maximizing therapeutic precision. Furthermore, tumor-targeted imaging facilitates diagnostic applications, such as preoperative tumor localization and postoperative detection of residual malignant cells [75,76]. For instance, nitrogen-rich mesoporous carbon nanospheres were synthesized using Triton-X as a structural template and pyrrole/aniline precursors. These luminescent hollow nanospheres combine PTT with fluorescence (FL) imaging capabilities, exhibiting a fluorescence quantum yield of 14.6%. The nanospheres induced potent thermal ablation of tumor cells, while their FL properties enabled real-time tracking of therapeutic responses [73]. Moreover, multimodal bioimaging, including different imaging platforms simultaneously, could improve the accuracy of imaging guidance and adjuvant therapy since the advantages and disadvantages of the different imaging modes complemented each other [75]. Pan et al. [74] have developed gadolinium-containing semiconductor polymer nanoparticles (SPN-Gd) that function as both an FL signal source and magnetic resonance imaging (MRI) contrast agents, thus offering a simplified nanotheranostic platform for efficient MRI/FL dual-modal imaging-guided PTT. Following intravenous administration of nanoparticles, FL signals were observed at the tumor site and progressively increased, peaking at 24 h and remaining elevated from 24 to 72 h. The maximum fluorescence signal of SPN-Gd detected at 24 h further implied that PTT should be performed 24 h following the injection of SPN-Gd. Furthermore, the biodistribution of SPN-Gd was assessed by FL imaging at 72 h post-injection, revealing the liver as having the highest fluorescence signal, followed by the tumor, spleen, and other major organs. (Figure 2B). Beyond MRI and FL, many imaging platforms—including computed tomography (CT) [54,75], light scattering imaging [64], and photoacoustic (PA) imaging [83]—have been synergized with PTAs to enhance diagnostic-therapeutic integration. The simultaneous use of diverse imaging platforms in multimodal bioimaging can improve the precision of imaging guidance and adjuvant therapy, as the advantages and disadvantages of different imaging modes are mutually compensating [75]. Noninvasive, real-time monitoring of treatment progres-

sion and feedback-driven adjustments are pivotal for translating preclinical successes into clinical practice. By bridging imaging precision with therapeutic spatiotemporal control, these advancements herald a new era of personalized oncology, where PTT is tailored to individual tumor dynamics and patient-specific pharmacokinetics.

## 3. Synergistic PTT-Based Therapies

The inherent diversity, complexity, and heterogeneity of tumors often render monotherapy insufficient for complete eradication [142]. To address this, combinatorial therapies can be strategically designed to exploit tumor and microenvironmental heterogeneity, integrating multiple modalities to achieve synergistic antitumor effects [85]. Such approaches enable comprehensive therapeutic outcomes while reducing individual treatment dosages without compromising efficacy—or even enhancing it [95,96]. PTT-based synergistic systems are particularly advantageous, as localized hyperthermia acts as a potent sensitizer by altering chemotherapeutic pharmacokinetics, modulating cell membrane permeability/stability, enhancing tissue oxygenation, and disrupting DNA repair mechanisms critical for tumor recovery [114–117]. These thermal-driven modifications amplify the cytotoxic effects of chemotherapy, immunotherapy, or radiotherapy, overcoming resistance mechanisms inherent to heterogeneous tumor subpopulations.

### 3.1. PTT Combined with PDT

PDT eliminates tumors by converting oxygen into reactive oxygen species (ROS) via photosensitizers (PS) under light irradiation. However, the hypoxic TME severely limits PDT efficacy, hindering its clinical application [143]. In contrast, PTT operates independently of oxygen availability and can synergistically enhance PDT through mild hyperthermia. Initial mild heating increases tumor blood flow and endothelial gaps, transiently improving oxygenation to enable effective PDT while enhancing nanocarrier delivery to tumors. Subsequent PDT following PTT thus achieves superior therapeutic outcomes [144]. ROS generated during PDT also sensitizes cancer cells to PTT-induced hyperthermia, creating a bidirectional therapeutic amplification loop [79]. Although some studies employ dual laser sources to activate PTT and PDT independently, this complicates clinical workflows [78]. Most research focuses on single-laser irradiation, which synchronizes PTT and PDT activation, minimizes treatment latency, and enhances synergy [139,145]. Photothermal nanoparticles can serve as PS carriers by matching their LSPR wavelength with the PS excitation spectrum, enabling single-laser excitation. In such systems, the intense near-field distribution generated by LSPR around plasmonic NPs (such as AuNPs) enhances PS excitation efficiency [80]. For example, Li et al. [85] fabricated a multifunctional Au@Pt-Ce6-HN-1 nanoplatform. They synthesized sea urchin-like Au@Pt nanozymes using a simple seed-mediated growth method and subsequently conjugated chlorin e6 (Ce6) and the HN-1 peptide (TSPLNIHNGQKL) to the Au@Pt surface via amide reactions. This platform exhibits exceptional photothermal and photodynamic performance, enabling synergistic PTT/PDT for enhanced tumor therapy (Figure 3A). Another nanoplatform that integrates indocyanine green (ICG) with hyaluronic acid-coated single-walled carbon nanotubes (SWCNT-HANPs) was developed to co-activate PTT and PDT. ICG's thermal stability ensures simultaneous photothermal and photodynamic effects under NIR irradiation [83]. These dual-modal systems exemplify the potential of rational nanomaterial design to overcome the intrinsic limitations of standalone therapies, offering a blueprint for next-generation combinatorial strategies.
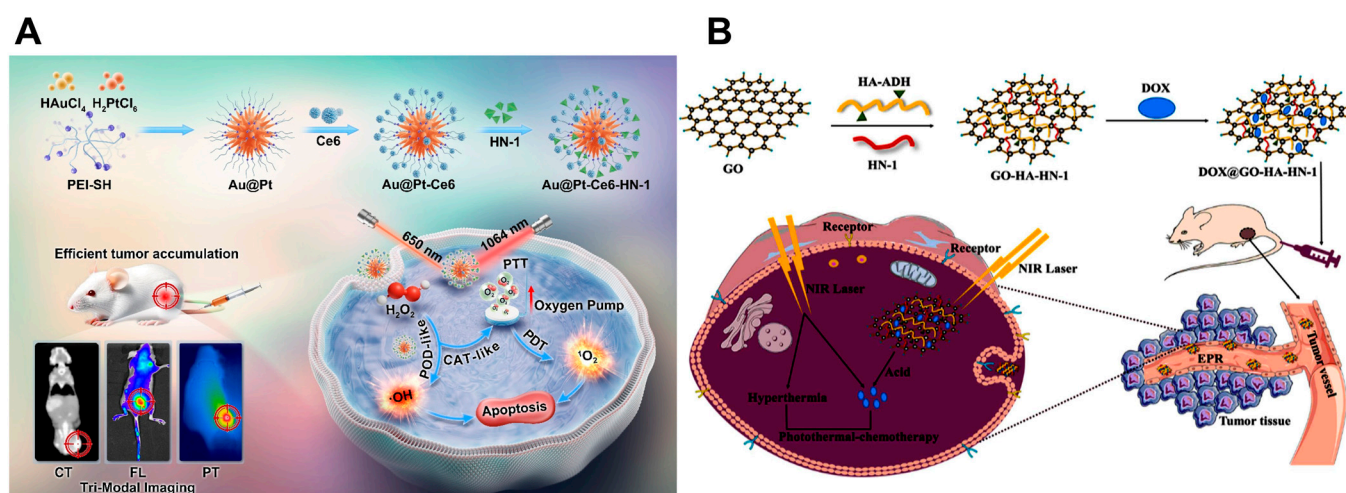
**Figure 3.** Synergistic PTT based therapies. (**A**) Schematic illustration of the key preparation steps for the Au@Pt-Ce6-HN-1 nanoplatform and its synergistic PTT/PDT antitumor mechanism. Reproduced with permission [85]. Copyright 2024, Elsevier Group (Amsterdam, The Netherlands). (**B**) Schematic illustration of the synthesis of dual-targeting nanoparticles DOX@GO-HA-HN-1 and their application in chemotherapy-synergized PTT for oral cancer. Reproduced with permission [94]. Copyright 2024, Elsevier Group (Amsterdam, The Netherlands).

### 3.2. PTT Combined with Chemotherapy

Chemotherapy employs cytotoxic agents to eliminate tumor cells, suppress proliferation, and eradicate residual malignancies [146]. However, systemic toxicity—such as myelosuppression, gastrointestinal distress, and alopecia—limits its clinical utility [147]. Thus, achieving on-demand controlled drug release is critical, requiring nanocarriers to balance premature drug leakage in circulation with rapid payload discharge at tumor sites. PTT has emerged as a potent external stimulus for tumor-specific and sequential drug release. Mechanisms include photothermal-mediated carrier disruption (e.g., thermal lysis of liposomes) or cleavage of thermolabile chemical bonds (e.g., Au-S bonds), with laser intensity modulating release kinetics [53]. Moreover, PTT remodels the TME by enhancing vascular permeability and interstitial fluid pressure, thereby promoting nanocarrier penetration and intratumoral accumulation [148]. The synergistic integration of PTT and chemotherapy amplifies therapeutic efficacy through dual pathways: (1) localized hyperthermia directly sensitizes cancer cells to chemotherapeutics, and (2) photothermally enhanced drug delivery enables the eradication of metastatic lesions beyond the irradiation field [55,149]. For example, Li et al. [94] have developed a novel dual-targeting nano-delivery system for the combined effects of PTT and chemotherapy through the co-modification of carboxylated graphene oxide (GO) with hyaluronic acid (HA) and HN-1 peptide followed by the encapsulation of the anticancer drug doxorubicin (DOX) (Figure 3B). Other exemplary systems include gold nanoflowers with DOX [99], gold nanorods conjugated to vincristine (VCR) [89], Prussian blue nanoparticles loaded with DOX [100], and ultrasmall gold nanoparticles complexed with cisplatin [91]. These platforms demonstrate superior antitumor outcomes by harmonizing photothermal ablation with spatiotemporally controlled chemotherapy.

### 3.3. PTT Combined with Radiotherapy

Radiotherapy (RT) employs high-energy ionizing radiation to eradicate cancer cells, commonly administered before or after surgical tumor resection to eliminate residual malignancies and prevent recurrence [150]. However, RT predominantly targets tumor cells in the G2/M phase, exhibiting limited efficacy against S-phase cells [151]. Its ther-

apeutic impact is further constrained by tumor hypoxia, a key contributor to post-RT relapse and metastasis [152,153]. Additionally, RT inflicts severe collateral damage on normal tissues exposed to ionizing radiation [154]. PTT synergistically enhances RT efficacy by improving tumor oxygenation through hyperthermia-induced blood flow augmentation. This combinatorial approach leverages the distinct anticancer mechanisms of RT and PTT to overcome therapeutic resistance. AuNPs, owing to their megavolt or kilovolt X-ray absorption properties, have emerged as novel radiosensitizers in preclinical studies [155]. Radiation enhancement by these agents is mediated by both physical dose deposition (through photoelectric and Compton interactions) and biological mechanisms such as amplifying oxidative stress, disrupting the cell cycle, and inhibiting DNA repair [156]. For instance, Neshastehriz et al. [103] synthesized folate-conjugated AuNPs (F-AuNPs) that selectively accumulate in tumors via folate receptor-mediated targeting. Under 532 nm laser irradiation, F-AuNPs induced significant thermal ablation due to their localized photothermal conversion. Simultaneously, their high Z-value enhanced radiosensitization during X-ray exposure. In cancer cells treated with F-AuNPs, dual irradiation (laser + X-ray) reduced cell viability, far exceeding the effects of PTT or RT alone. This dramatic synergy underscores the potential of AuNP-mediated RT-PTT integration to achieve precision tumor eradication while sparing healthy tissues.

### 3.4. PTT Combined with Gene Therapy

Gene therapy can induce apoptosis in malignant cells and downregulate heat shock protein (HSP) expression to mitigate cellular protection against photothermal-induced hyperthermia or upregulate cytotoxic immune cytokines [157]. Researchers have employed gene silencing to counteract thermoresistance caused by the heat shock response (HSR) and synergized this strategy with PTT for treating OSCC [158]. The HSR, a defense mechanism triggered by thermal or other stressors, involves adaptive gene expression changes that enhance cancer cell resistance to therapeutic heat, thereby diminishing PTT efficacy [159]. To address this, small interfering RNA (siRNA) has been utilized to inhibit HSR signaling, which is mediated by HSPs such as HSP70 [57] and BAG3 [104,160]. For instance, Wang et al. [104] developed a gold nanorod-siRNA (GNRs-siRNA) platform with gene-silencing capabilities. This nanoplatform sensitizes cancer cells to PTT using moderate laser irradiation by downregulating BAG3 expression and promoting apoptosis, effectively overcoming thermoresistance. GNRs-siRNA-mediated PTT eliminates therapeutic resistance via targeted gene silencing, amplifies photothermal efficacy, and maximizes tumor eradication while minimizing off-target tissue damage, demonstrating significant potential for clinical translation in precision oncology.

### 3.5. PTT Combined with Immunotherapy

Immunotherapy harnesses the intrinsic capacity of the cellular and humoral immune systems to target and eliminate tumor cells directly, offering high therapeutic specificity and safety [161]. Current strategies to stimulate antitumor immunity include checkpoint blockade therapy, adoptive T cell transfer, and cancer vaccines [162,163]. By enhancing the maturation of antigen-presenting cells (APCs) and cytotoxic T lymphocytes (CTLs) and suppressing immunosuppressive mechanisms within tumors, immunoadjuvants or checkpoint inhibitors amplify immune activation [162]. The integration of PTT with immunotherapy creates synergistic anticancer effects through dual mechanisms: (1) PTT-induced immunogenic cell death releases tumor-specific antigens in situ, priming adaptive antitumor immune responses and constraining tumor growth by eliciting immunogenic cell death, (2) host immune activation eradicates disseminated or metastatic lesions beyond the laser-irradiated tumor field, preventing recurrence [53]. For example, Bu et al. [105]

synthesized matrix metalloproteinase (MMP)-degradable gelatin nanoparticles (GNPs) co-loaded with ICG and a signal transducer activator of transcription 3 (STAT3) inhibitor (NSC74859) to construct Gel-N-ICG NPs. The released NSC inhibits immune checkpoint proteins and induces robust antitumor immunity, significantly suppressing tumor growth. Under NIR irradiation, Gel-N-ICG NPs simultaneously mediate photothermal ablation and immune checkpoint blockade, achieving combinatorial tumor eradication and systemic immune memory. High cholesterol in the TME may affect T cells' function, leading to the depletion of $CD8^+$ T cells' immune function and other functional abnormalities. Song et al. [115] developed a cholesterol-regulating nanoplatform comprised of simvastatin (SIM) encapsulated within chlorin e6-polyethylene glycol (Ce6-PEG). Simvastatin acts by inhibiting hydroxy-3-methylglutaryl-CoA reductase (HMGCR), thereby lowering cholesterol levels in tumor tissues and reversing the immunosuppressive effects of tumor-infiltrating T cells. It unlocked new paradigms to provide a TME-regulated-based scaffold for practical cancer applications.

## 4. PTT-Based Multifunctional Therapeutic Platform

Currently, surgical resection remains the primary treatment for oral cancer. However, residual tumor cells at surgical margins frequently lead to recurrence [164]. Occurrence of positive surgical margins, indicating residual malignant cells, is reported in 20–50% of OSCC cases—a frequency 1.7 times higher compared to other head and neck locations—which continues to hinder the attainment of favorable postoperative outcomes [165–167]. Adjuvant therapies, such as radiotherapy and chemotherapy, are often required to eliminate residual tumor cells but are associated with severe side effects, including osteoradionecrosis and rampant caries, which profoundly impair patients' quality of life [168,169]. Moreover, extensive bone and soft tissue defects caused by surgery compromise aesthetic and functional outcomes (such as mastication, speech), imposing significant psychological and physiological burdens [170,171]. Autologous tissue transplantation, the clinical "gold standard" for defect repair, faces limitations such as donor site morbidity, postsurgical hair growth in flaps, and technical complexity [172–175]. Thus, eliminating residual tumor cells while promoting tissue regeneration is critical in postoperative care. Demonstrated in the treatment of infectious bone defects, NIR-mediated mild hyperthermia enhances cell proliferation, differentiation, and local blood flow, enabling PTT to function as a postoperative adjunct for eradicating residual tumor cells and stimulating tissue repair [176–179]. In addition, surgical exposure of the tumor region adds to its advantages. However, standalone PTT exhibits limited regenerative capacity [180]. Recent advances in tissue engineering have spurred interest in integrating PTT with biomimetic scaffolds to construct multifunctional systems that synergize antitumor efficacy and tissue regeneration [181–183].

Bioinspired scaffolds are emerging as promising platforms for oral wound repair [184]. These scaffolds provide structural guidance for cell migration and proliferation, facilitating tissue formation. Medical-grade silk fibroin (SF), renowned for its biocompatibility, elasticity, and tunable biodegradability, is widely employed in scaffold design [185]. Collagen (COL) further enhances scaffold performance by promoting platelet adhesion, fibroblast proliferation, and angiogenesis during early wound healing [186]. Three-dimensional printing enables the fabrication of personalized scaffolds with interconnected macroporous architectures tailored to irregular defects. Accordingly, many research efforts have focused on developing 3D-printed biomimetic scaffolds composed of SF/COL [57]. For instance, PTT and tissue engineering scaffold were rationally integrated to construct a $Ti_3C_2$ MXene, COL, SF, and quercetin composite scaffold (M-CSQ), a 3D printed biomaterial that simultaneously kills OSCC cells and promotes the regeneration of the mucosal defects. The

M-CSQ scaffolds were prepared using cryogenic 3D printing and freeze-drying techniques, with sufficient pores that allow abundant cell migration and provide a proliferation space. The results suggest the achievement of concurrent residual OSCC cell elimination and oral mucosal wound repair (Figure 4A) [57]. Short-term, controlled laser exposure during PTT minimally impacts long-term mucosal regeneration, underscoring its clinical feasibility [58]. In advanced oral cancers invading maxillofacial bone, surgical ablation often results in critical-sized defects requiring reconstruction. Nanohydroxyapatite (nHA)-incorporated scaffolds, mimicking bone's inorganic composition, offer osteoconductivity and mechanical robustness [187,188]. To simultaneously eradicate residual tumor cells and regenerate bone, a 3D-printed collagen-silk-nHA (CSH) scaffold was functionalized with MXene nanosheets (M-CSH) [56]. Both the CSH and M-CSH scaffolds were shown to support the generation of new bone, with the M-CSH scaffolds exhibiting a superior ability to form bone compared to the CSH scaffolds, even with short-term PTT (Figure 4B). This indicates that short-term PTT does not adversely impact long-term bone repair outcomes. Although localized heat from NIR irradiation may transiently affect adjacent osteocytes, bone marrow mesenchymal stem cells (BMSCs) recruited during the inflammatory phase migrate into scaffold pores, proliferate, and differentiate, ultimately restoring osseous architecture. Notably, PTT-induced inflammation mirrors the initial bone healing phase, enhancing BMSC homing to defect sites [189].
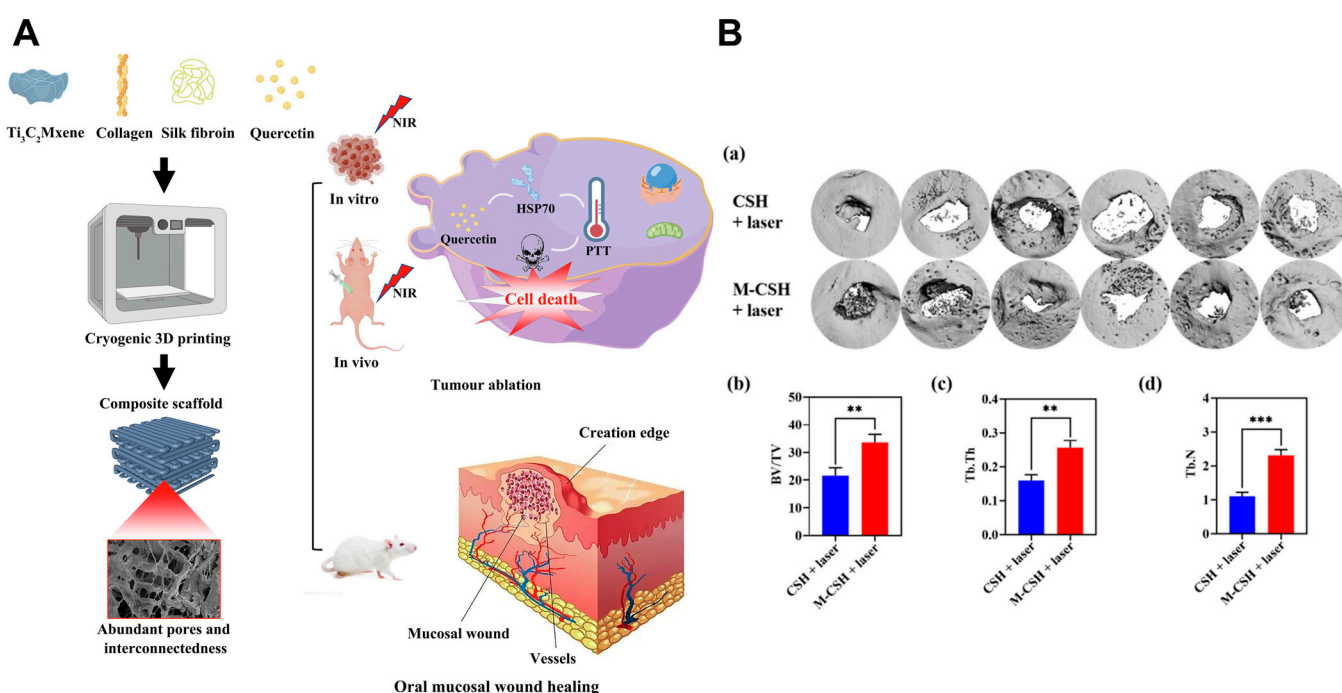


**Figure 4.** PTT based multifunctional therapeutic platform. (**A**) Illustration outlining the preparation scheme of M-CSQ scaffolds and their role in combinational PTT against oral cancer cells and oral mucosal wound repair. Reproduced with permission [57]. Copyright 2023, Elsevier Group (Amsterdam, The Netherlands). (**B**) Osteogenesis performance of CSH and M-CSH scaffolds. (**a**) Micro-CT images of mandibular defect areas at 8 weeks after surgery, the value of (**b**) BV/TV, (**c**) Tb. Th and (**d**) Tb. N in new bone tissue. ** $p < 0.01$, *** $p < 0.001$. Reproduced under the terms of the Creative Commons CC BY license [56]. Copyright 2021, The Author(s). Published by Oxford University Press (Oxford, UK).

## 5. PTT for OPMDs Management

Oral potentially malignant disorders (OPMDs)—including conditions such as leukoplakia, erythroplakia, oral lichen planus, proliferative verrucous leukoplakia, and oral

submucous fibrosis—significantly increase the risk of OSCC development [14]. Current clinical management strategies for OPMDs encompass surgical resection, cryotherapy, laser ablation, PDT, and pharmacotherapy [190]. However, anatomical and functional constraints in the orofacial region often limit the applicability of invasive modalities like surgery or laser therapy [119]. With its minimally invasive nature, high selectivity, repeatability, and minimal scarring, PTT has emerged as an indispensable approach for treating OPMDs, particularly in functionally sensitive areas.

Currently, PTT applications in OPMDs remain limited, primarily focusing on oral leukoplakia (OLK)—the most prevalent OPMD, defined as a non-removable, non-scrapable white plaque with malignant potential [29,191]. OLK exhibits a 3.5% prevalence rate, with 4–13% progressing to malignancy [192,193]. Preventing OPMD-to-OSCC transformation is critical. For instance, ITIC-Th, a dual-modal PDT/PTT agent, synergistically induces cell death by downregulating tumor-associated biomarkers (such as ALDH1, p53, cyclin D1, PDCD5, and PDPN) in vitro, effectively blocking malignant transformation and promoting OLK lesion regression. Concurrently, PTT enhances local blood flow to accelerate tissue healing (Figure 5A) [115]. Nevertheless, nonspecific thermal diffusion during PTT risks collateral damage to adjacent healthy tissues. To address this, fibroblast activation protein (FAP)—overexpressed in epithelial tumors and inflammatory lesions but absent in normal adult tissues—has been leveraged to design FAP-targeted nanodrug delivery systems (Figure 5B) [119]. Soluble microneedles have also been used as in situ transdermal delivery systems to decrease the risk of damage to surrounding normal tissue [120]. These systems achieve localized therapy by selectively accumulating in lesions, maximizing therapeutic precision while minimizing off-target effects.
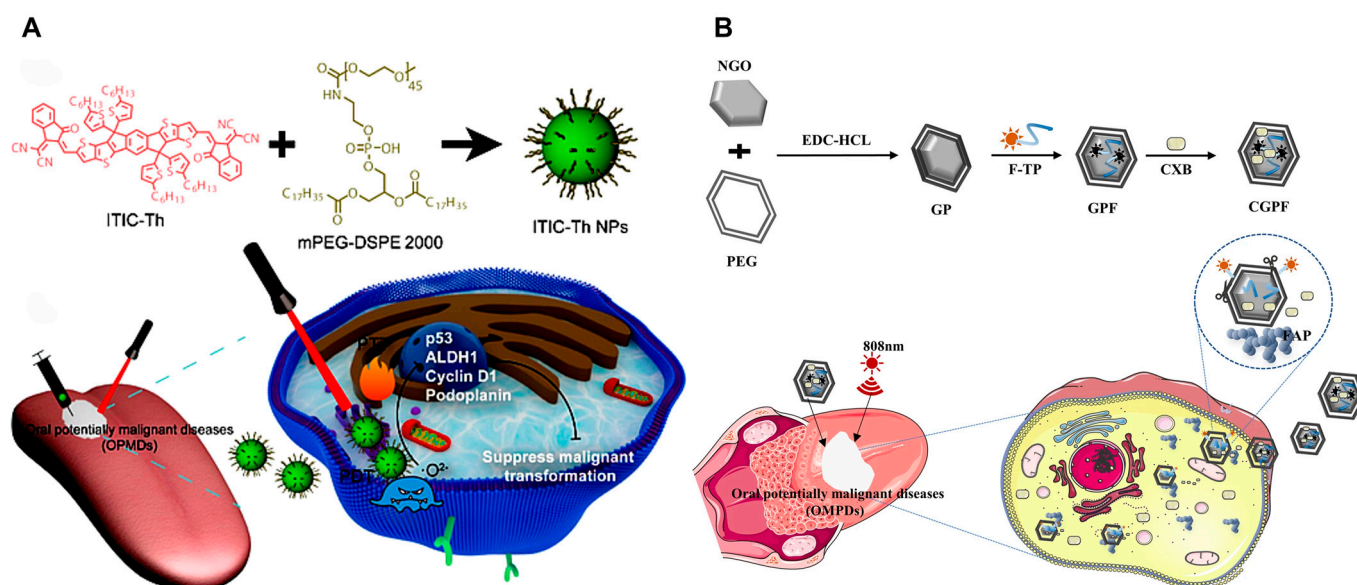


**Figure 5.** PTT for oral potentially malignant disorders (OPMDs) management. (**A**) Schematic illustration of the synthesis of ITIC-Th NPs and their synergistic PDT/PTT mechanism. Reproduced under the terms of the Creative Commons CC BY license [118]. Copyright 2022, The Author(s). Published by Springer Nature Group (Berlin, Germany). (**B**) Illustration depicting the synthesis of the nano-drug delivery system and describing the combined PTT approach. Reproduced with permission [119]. Copyright 2023, Springer Nature Group (Berlin, Germany).

## 6. Summary and Outlook

PTT has emerged as a promising anticancer modality owing to its non-invasive nature, precise spatiotemporal control, and resistance-free mechanism, offering transformative potential for both the prevention and treatment of oral cancer. Advances in nanotechnol-

ogy have driven the rational design of PTAs through material selection, morphological optimization, and size modulation to maximize PCE and therapeutic outcomes. Concurrently, strategies to enhance the tumor-specific accumulation of PTAs—via active targeting (e.g., ligand-receptor interactions) and image-guided timing of laser irradiation—have significantly improved treatment precision. The integration of PTT with multimodal therapies, including conventional approaches (surgery, radiotherapy, chemotherapy) and emerging modalities (gene therapy, PDT, immunotherapy), addresses the limitations of monotherapy by leveraging synergistic effects. For instance, PTT-induced hyperthermia sensitizes tumors to chemotherapy while mitigating systemic toxicity, and combinational PTT-immunotherapy eradicates metastatic lesions via systemic immune activation. Notably, the fusion of PTT with tissue-engineered scaffolds represents a groundbreaking approach, enabling simultaneous tumor ablation and functional tissue regeneration—a critical advancement for reconstructing maxillofacial defects post-resection. While this review categorizes PTT strategies individually, real-world applications often combine multiple approaches (e.g., targeted PTAs + image guidance + scaffold integration) to amplify efficacy [96,98]. Furthermore, strategies developed for oral cancer—such as optimized PTA design and combinatorial regimens—hold untapped potential for OPMDs, given the shared therapeutic vulnerabilities between OPMDs and malignant cells.

Despite the preclinical success, clinical translation faces challenges: (1) Limited ablation efficacy in bulky tumors, (2) Safety concerns regarding systemic nanomaterial administration, (3) Reliance on cell line-derived xenograft models, which poorly replicate human tumor heterogeneity and microenvironmental complexity. Future efforts should prioritize (1) Developing PTAs with high extinction coefficients and optimal absorption/scattering ratios for NIR-II window (1000–1700 nm) applications, which offer deeper tissue penetration and higher permissible irradiation doses. (2) Exploring localized delivery systems (e.g., hydrogels, nanocapsules, hyaluronic acid-based carriers) to minimize systemic toxicity. (3) Adopting patient-derived xenograft (PDX) models to predict clinical outcomes better. (4) Investigating mechanisms underlying mild hyperthermia-driven tissue regeneration, currently attributed to exogenous factor release but lacking mechanistic depth. (5) Accelerating clinical trials to validate preclinical findings, as current human studies remain scarce. In conclusion, PTT stands at the frontier of oral oncology, with transformative potential to bridge tumor eradication and functional restoration. Through interdisciplinary innovation and rigorous clinical validation, PTT-based paradigms may soon redefine standards of care for oral cancer and OPMDs.

**Conflicts of Interest:** The authors declare no conflicts of interest.

# Abbreviations

The following abbreviations are used in this manuscript:

| | |
|---|---|
| 3D | Three-dimensional |
| 4NQO | 4-nitroquinoline 1-oxide |
| APCs | Antigen-presenting cells |
| AuNPs | Au nanoparticles |
| AuNRs | Au nanorods |
| BMSCs | Bone marrow mesenchymal stem cells |
| BP | Black phosphorus |
| BSA | Bovine serum albumin |
| CDX | Cell line-derived xenograft |
| Ce6 | Chlorin e6 |
| COL | Collagen |
| CT | Computed tomography |
| CTAB | Cetyltrimethylammonium bromide |
| CTLs | Cytotoxic T lymphocytes |
| DMBA | 7,12-dimethylbenz[a]anthracene |
| DOX | Doxorubicin |
| DDS | Drug delivery systems |
| EGFR | Epithelial growth factor receptor |
| EPR | Enhanced permeability and retention |
| FAP | Fibroblast activation protein |
| FL | Fluorescence imaging |
| GNR | Gold nanorod |
| GO | Graphene oxide |
| HA | Hyaluronic acid |
| HBP | Hamster buccal pouch |
| HMPBs | Hollow meso-porous Prussian blue NPs |
| HNSCC | Head and neck squamous cell carcinoma |
| HSP | Heat shock protein |
| HSR | Heat shock response |
| ICG | Indocyanine green |
| KBV | Human oral epithelial carcinoma vincristine-resistant tumor |
| LSPR | Localized surface plasmon resonance |
| MMP | Matrix metalloproteinase |
| mPTT | Mild-temperature photothermal therapy |
| MRI | Magnetic resonance imaging |
| nHA | Nanohydroxyapatite |
| NIR | Near-infrared |
| NPs | Nanoparticles |
| NSs | Nanosheets |
| OLK | Oral leukoplakia |
| OPMDs | Oral potentially malignant disorders |
| OSCC | Oral squamous cell carcinoma |
| PA | Photoacoustic |
| PDA | Polydopamine |
| PDT | Photodynamic therapy |
| PEG | Poly(ethylene glycol) |
| PLGA | Poly(lactic-co-glycolic acid) |
| PLTs | Platelets |
| PPTT | Plasmonic photothermal therapy |

| PTT | Photothermal therapy |
|---|---|
| *P. gingivalis* | *Porphyromonas gingivalis* |
| PS | Photosensitizers |
| PT | Photothermal |
| PTAs | Photothermal agents |
| PTT | Photothermal therapy |
| RB | Rose bengal |
| ROS | Reactive oxygen species |
| RT | Radiotherapy |
| SF | Silk fibroin |
| SIM | Simvastatin |
| siRNA | Small interfering RNA |
| STAT3 | Signal transducer activator of transcription 3 |
| SWCNTs | Single-walled carbon nanotubes |
| TME | Tumor microenvironment |
| VCR | Vincristine |

# References

1. Spanemberg, J.C.; Cardoso, J.A.; Slob, E.M.G.B.; López-López, J. Quality of life related to oral health and its impact in adults. *J. Stomatol. Oral Maxillofac. Surg.* **2019**, *120*, 234–239. [CrossRef]

2. Coletta, R.D.; Yeudall, W.A.; Salo, T. Current trends on prevalence, risk factors and prevention of oral cancer. *Front. Oral Health* **2024**, *5*, 1505833. [CrossRef]

3. Balaji, H.; Aithal, V.U.; Varghese, J.J.; Devaraja, K.; Kumar, A.N.N. Agreement between patient-reported and clinician-rated speech and swallowing outcomes—Understanding the trend in post-operative oral cavity cancer patients. *Oral Oncol.* **2024**, *159*, 107068. [CrossRef]

4. Kijowska, J.; Grzegorczyk, J.; Gliwa, K.; Jędras, A.; Sitarz, M. Epidemiology, Diagnostics, and Therapy of Oral Cancer—Update Review. *Cancers* **2024**, *16*, 3156. [CrossRef]

5. Bray, F.; Laversanne, M.; Sung, H.; Ferlay, J.; Siegel, R.L.; Soerjomataram, I.; Jemal, A. Global cancer statistics 2022: GLOBOCAN estimates of incidence and mortality worldwide for 36 cancers in 185 countries. *CA-Cancer J. Clin.* **2024**, *74*, 229–263. [CrossRef]

6. Bray, F.; Ferlay, J.; Soerjomataram, I.; Siegel, R.L.; Torre, L.A.; Jemal, A. Global cancer statistics 2018: GLOBOCAN estimates of incidence and mortality worldwide for 36 cancers in 185 countries. *CA-Cancer J. Clin.* **2018**, *68*, 394–424. [CrossRef]

7. Sung, H.; Ferlay, J.; Siegel, R.L.; Laversanne, M.; Soerjomataram, I.; Jemal, A.; Bray, F. Global Cancer Statistics 2020: GLOBOCAN Estimates of Incidence and Mortality Worldwide for 36 Cancers in 185 Countries. *CA-Cancer J. Clin.* **2021**, *71*, 209–249. [CrossRef]

8. Tota, J.E.; Engels, E.A.; Lingen, M.W.; Agrawal, N.; Kerr, A.R.; Zumsteg, Z.S.; Cheung, L.C.; Katki, H.A.; Abnet, C.C.; Chaturvedi, A.K. Inflammatory Tongue Conditions and Risk of Oral Tongue Cancer Among the US Elderly Individuals. *J. Clin. Oncol.* **2024**, *42*, 1745–1753. [CrossRef]

9. Rumgay, H.; Nethan, S.T.; Shah, R.; Vignat, J.; Ayo-Yusuf, O.; Chaturvedi, P.; Guerra, E.N.S.; Gupta, P.C.; Gupta, R.; Liu, S.; et al. Global burden of oral cancer in 2022 attributable to smokeless tobacco and areca nut consumption: A population attributable fraction analysis. *Lancet Oncol.* **2024**, *25*, 1413–1423. [CrossRef]

10. Zahiruddin, Q.S.; Jena, D.; Ballal, S.; Kumar, S.; Bhat, M.; Sharma, S.; Kumar, M.R.; Rustagi, S.; Gaidhane, A.M.; Jain, L.; et al. Burden of oral cancer and associated risk factors at national and state levels: A systematic analysis from the global burden of disease in India, 1990–2021. *Oral Oncol.* **2024**, *159*, 107063.

11. Piemonte, E.D.; Lazos, J.P.; Gilligan, G.M.; Panico, R.L.; Werner, L.C.; Yang, Y.-H.; Warnakulasuriya, S. Chronic mechanical irritation enhances the effect of tobacco and alcohol on the risk of oral squamous cell carcinoma: A case-control study in Argentina. *Clin. Oral Investig.* **2022**, *26*, 6317–6326. [CrossRef]

12. Nokovitch, L.; Maquet, C.; Crampon, F.; Taihi, I.; Roussel, L.-M.; Obongo, R.; Virard, F.; Fervers, B.; Deneuve, S. Oral Cavity Squamous Cell Carcinoma Risk Factors: State of the Art. *J. Clin. Med.* **2023**, *12*, 3264. [CrossRef]

13. Warnakulasuriya, S. Oral potentially malignant disorders: A comprehensive review on clinical aspects and management. *Oral Oncol.* **2020**, *102*, 104550. [CrossRef]

14. Warnakulasuriya, S.; Kujan, O.; Aguirre-Urizar, J.M.; Bagan, J.V.; González-Moles, M.Á.; Kerr, A.R.; Lodi, G.; Mello, F.W.; Monteiro, L.; Ogden, G.R.; et al. Oral potentially malignant disorders: A consensus report from an international seminar on nomenclature and classification, convened by the WHO Collaborating Centre for Oral Cancer. *Oral Dis.* **2021**, *27*, 1862–1880. [CrossRef]

15. Villa, A.; Lodolo, M.; Ha, P. Oncological Outcomes of Patients With Oral Potentially Malignant Disorders. *JAMA Otolaryngol.–Head Neck Surg.* **2025**, *151*, 65–71. [CrossRef]

16. Kerr, A.R.; Lodi, G. Management of oral potentially malignant disorders. *Oral Dis.* **2021**, *27*, 2008–2025. [CrossRef]

17. Neville, B.W.; Day, T.A. Oral cancer and precancerous lesions. *CA-Cancer J. Clin.* **2002**, *52*, 195–215. [CrossRef]

18. Tan, Y.; Wang, Z.; Xu, M.; Li, B.; Huang, Z.; Qin, S.; Nice, E.C.; Tang, J.; Huang, C. Oral squamous cell carcinomas: State of the field and emerging directions. *Int. J. Oral Sci.* **2023**, *15*, 44. [CrossRef]

19. Matos, L.L.; Guimarães, Y.L.M.; Leite, A.K.; Cernea, C.R. Management of Stage III Oral Cavity Squamous Cell Carcinoma in Light of the New Staging System: A Critical Review. *Curr. Oncol. Rep.* **2023**, *25*, 107–113. [CrossRef]

20. Fan, H.-Y.; Zhu, Z.-L.; Zhang, W.-L.; Yin, Y.-J.; Tang, Y.-L.; Liang, X.-H.; Zhang, L. Light stimulus responsive nanomedicine in the treatment of oral squamous cell carcinoma. *Eur. J. Med. Chem.* **2020**, *199*, 112394. [CrossRef]

21. Pan, Q.; Tang, H.; Xie, L.; Zhu, H.; Wu, D.; Liu, R.; He, B.; Pu, Y. Recent advances in phototherapeutic nanosystems for oral cancer. *J. Mater. Chem. B* **2024**, *12*, 11560–11572. [CrossRef]

22. Shamsi, U.; Khan, M.A.A.; Qadir, M.S.; Rehman, S.S.U.; Azam, I.; Idress, R. Factors associated with the survival of oral cavity cancer patients: A single institution experience from Karachi, Pakistan. *BMC Oral Health* **2024**, *24*, 1427. [CrossRef]

23. Wei, L.-Y.; Li, Z.-Z.; Xu, Z.-Y.; Wang, G.-R.; Xiao, Y.; Liu, B.; Bu, L.-L. The ending is not the end: Lymph node metastasis in oral squamous cell carcinoma. *Int. Immunopharmacol.* **2025**, *146*, 113917. [CrossRef]

24. Alfertshofer, M.; Knoedler, L.; Mrosk, F.; Schmitz, A.; Richter, M.; Rendenbach, C.; Doll, C.; Heiland, M.; Koerdt, S. Histopathological invasion patterns and prognosis in Oral Squamous Cell Carcinoma: A retrospective analysis of 560 cases. *Oral Oncol.* **2025**, *163*, 107247. [CrossRef]

25. Li, S.S.; Wu, C.Z.; Li, L.J. Progress on photodynamic therapy in oral diseases. *West China J. Stomatol.* **2021**, *39*, 215–220.

26. Wu, Y.; Li, X.; Liu, H.; Yang, X.; Li, R.; Zhao, H.; Shang, Z. Organoids in the oral and maxillofacial region: Present and future. *Int. J. Oral Sci.* **2024**, *16*, 61. [CrossRef]

27. Cheng, Q.-S.; Xu, P.-Y.; Luo, S.-C.; Chen, A.-Z. Advances in Adhesive Materials for Oral and Maxillofacial Soft Tissue Diseases. *Macromol. Biosci.* **2025**, *25*, 2400494. [CrossRef]

28. Chamoli, A.; Gosavi, A.S.; Shirwadkar, U.P.; Wangdale, K.V.; Behera, S.K.; Kurrey, N.K.; Kalia, K.; Mandoli, A. Overview of oral cavity squamous cell carcinoma: Risk factors, mechanisms, and diagnostics. *Oral Oncol.* **2021**, *121*, 105451. [CrossRef]

29. Gates, J.C.; Abouyared, M.; Shnayder, Y.; Farwell, D.G.; Day, A.; Alawi, F.; Moore, M.; Holcomb, A.J.; Birkeland, A.; Epstein, J. Clinical Management Update of Oral Leukoplakia: A Review From the American Head and Neck Society Cancer Prevention Service. *Head Neck-J. Sci. Spec. Head Neck* **2025**, *47*, 733–741. [CrossRef]

30. Niu, Q.; Sun, Q.; Bai, R.; Zhang, Y.; Zhuang, Z.; Zhang, X.; Xin, T.; Chen, S.; Han, B. Progress of Nanomaterials-Based Photothermal Therapy for Oral Squamous Cell Carcinoma. *Int. J. Mol. Sci.* **2022**, *23*, 10428. [CrossRef]

31. Zhuoping, Z.; Pengfei, X.; Yang, G.; Caifeng, Z.; Kuanshou, Z.; Qingmei, L. Research progress on the use of photothermal therapy to treat oral squamous cell carcinoma. *Int. J. Stomatol.* **2022**, *49*, 462–470.

32. Hare, J.I.; Lammers, T.; Ashford, M.B.; Puri, S.; Storm, G.; Barry, S.T. Challenges and strategies in anti-cancer nanomedicine development: An industry perspective. *Adv. Drug Deliv. Rev.* **2017**, *108*, 25–38. [CrossRef]

33. Cao, L.; Wu, Y.; Shan, Y.; Tan, B.; Liao, J. A review: Potential application and outlook of photothermal therapy in oral cancer treatment. *Biomed. Mater.* **2022**, *17*, 022008. [CrossRef]

34. Montero, P.H.; Patel, S.G. Cancer of the oral cavity. *Surg. Oncol. Clin. N. Am.* **2015**, *24*, 491–508. [CrossRef]

35. Lu, Q.; Yu, J.; Zhou, Y.; Zhang, Z.; Guo, L.; Bi, X. Prediction of postoperative dysphagia in patients with oral cancer: A prospective cohort study. *J. Stomatol. Oral Maxillofac. Surg.* **2024**, *125* (Suppl. S2), 101957. [CrossRef]

36. Shirakawa, J.; Kaneuji, T.; Matsuno, D.; Nagata, J.; Hirayama, B.; Tanaka, F.; Nakamura, Y.; Yamashita, Y. Correlation during the extent of surgical resection, oral function and quality of life after tongue cancer surgery: Single-institution study. *J. Stomatol. Oral Maxillofac. Surg.* **2024**, *125*, 101907. [CrossRef]

37. Goetz, J.W.; Rabinowits, G.; Kalman, N.; Villa, A. A Review of Immunotherapy for Head and Neck Cancer. *J. Dent. Res.* **2024**, *103*, 1185–1196. [CrossRef]

38. Mitea, G.; Schröder, V.; Iancu, I.M.; Mireșan, H.; Iancu, V.; Bucur, L.A.; Badea, F.C. Molecular Targets of Plant-Derived Bioactive Compounds in Oral Squamous Cell Carcinoma. *Cancers* **2024**, *16*, 3612. [CrossRef]

39. Chen, J.; Xu, X.; Wang, K.; Xue, M.; Wang, Q.; Zhong, W.; Wan, Y.; Liu, X.; Zheng, J.; Gao, G.; et al. Hypoxia-Activated Liposomes Enable Synergistic Photodynamic Therapy for Oral Cancer. *Adv. Healthc. Mater.* **2025**, *14*, e2404395. [CrossRef]

40. Nandini, D.B.; Rao, R.S.; Hosmani, J.; Khan, S.; Patil, S.; Awan, K.H. Novel therapies in the management of oral cancer: An update. *Dis. Mon.* **2020**, *66*, 101036. [CrossRef]

41. Wei, Y.; Wang, Z.; Yang, J.; Xu, R.; Deng, H.; Ma, S.; Fang, T.; Zhang, J.; Shen, Q. Reactive oxygen species/photothermal therapy dual-triggered biomimetic gold nanocages nanoplatform for combination cancer therapy via ferroptosis and tumor-associated macrophage repolarization mechanism. *J. Colloid Interface Sci.* **2022**, *606*, 1950–1965. [CrossRef]

42. Yu, S.; Xia, G.; Yang, N.; Yuan, L.; Li, J.; Wang, Q.; Li, D.; Ding, L.; Fan, Z.; Li, J. Noble Metal Nanoparticle-Based Photothermal Therapy: Development and Application in Effective Cancer Therapy. *Int. J. Mol. Sci.* **2024**, *25*, 5632. [CrossRef] [PubMed]

43. Gai, S.; Yang, G.; Yang, P.; He, F.; Lin, J.; Jin, D.; Xing, B. Recent advances in functional nanomaterials for light–triggered cancer therapy. *Nano Today* **2018**, *19*, 146–187. [CrossRef]

44. Li, X.; Lovell, J.F.; Yoon, J.; Chen, X. Clinical development and potential of photothermal and photodynamic therapies for cancer. *Nat. Rev. Clin. Oncol.* **2020**, *17*, 657–674. [CrossRef]

45. Ren, S.; Cheng, X.; Chen, M.; Liu, C.; Zhao, P.; Huang, W.; He, J.; Zhou, Z.; Miao, L. Hypotoxic and Rapidly Metabolic PEG-PCL-C3-ICG Nanoparticles for Fluorescence-Guided Photothermal/Photodynamic Therapy against OSCC. *ACS Appl. Mater. Interfaces* **2017**, *9*, 31509–31518. [CrossRef] [PubMed]

46. Ma, L.; Feng, X.; Liang, H.; Wang, K.; Song, Y.; Tan, L.; Wang, B.; Luo, R.; Liao, Z.; Li, G.; et al. A novel photothermally controlled multifunctional scaffold for clinical treatment of osteosarcoma and tissue regeneration. *Mater. Today* **2020**, *36*, 48–62. [CrossRef]

47. Wu, M.; Liu, H.; Li, D.; Zhu, Y.; Wu, P.; Chen, Z.; Chen, F.; Chen, Y.; Deng, Z.; Cai, L. Smart-Responsive Multifunctional Therapeutic System for Improved Regenerative Microenvironment and Accelerated Bone Regeneration via Mild Photothermal Therapy. *Adv. Sci.* **2024**, *11*, 2304641. [CrossRef]

48. Lan, J.; Zeng, R.; Li, Z.; Yang, X.; Liu, L.; Chen, L.; Sun, L.; Shen, Y.; Zhang, T.; Ding, Y. Biomimetic Nanomodulators With Synergism of Photothermal Therapy and Vessel Normalization for Boosting Potent Anticancer Immunity. *Adv. Mater.* **2024**, *36*, 2408511. [CrossRef]

49. Gao, J.; Qin, H.; Wang, F.; Liu, L.; Tian, H.; Wang, H.; Wang, S.; Ou, J.; Ye, Y.; Peng, F.; et al. Hyperthermia-triggered biomimetic bubble nanomachines. *Nat. Commun.* **2023**, *14*, 4867. [CrossRef]

50. Chen, G.; Yang, Z.; Yu, X.; Yu, C.; Sui, S.; Zhang, C.; Bao, C.; Zeng, X.; Chen, Q.; Peng, Q. Intratumor delivery of amino-modified graphene oxide as a multifunctional photothermal agent for efficient antitumor phototherapy. *J. Colloid Interface Sci.* **2023**, *652*, 1108–1116. [CrossRef]

51. Jiang, Y.; Tan, Z.; Zhao, T.; Wu, J.; Li, Y.; Jia, Y.; Peng, Z. Indocyanine green derived carbon dots with significantly enhanced properties for efficient photothermal therapy. *Nanoscale* **2023**, *15*, 1925–1936. [CrossRef] [PubMed]

52. Li, H.; Li, P.; Zhang, J.; Lin, Z.; Bai, L.; Shen, H. Applications of nanotheranostics in the second near-infrared window in bioimaging and cancer treatment. *Nanoscale* **2024**, *16*, 21697–21730. [CrossRef]

53. Liu, Y.; Bhattarai, P.; Dai, Z.; Chen, X. Photothermal therapy and photoacoustic imaging via nanotheranostics in fighting cancer. *Chem. Soc. Rev.* **2019**, *48*, 2053–2108. [CrossRef]

54. Hao, M.; Li, X.; Zhang, X.; Tao, B.; Shi, H.; Wu, J.; Li, Y.; Li, X.; Li, S.; Wu, H.; et al. Tongue squamous cell carcinoma-targeting Au-HN-1 nanosystem for CT imaging and photothermal therapy. *Int. J. Oral Sci.* **2025**, *17*, 9. [CrossRef]

55. Li, H.; Zhu, L.; Zhang, Y.; Yang, L.; Wu, W.; Yang, D. Biomimetic nanotherapeutics for homotypic-targeting photothermal/chemotherapy of oral cancer. *J. Control. Release* **2024**, *366*, 28–43. [CrossRef] [PubMed]

56. Li, F.; Yan, Y.; Wang, Y.; Fan, Y.; Zou, H.; Liu, H.; Luo, R.; Li, R.; Liu, H. A bifunctional MXene-modified scaffold for photothermal therapy and maxillofacial tissue regeneration. *Regen. Biomater.* **2021**, *8*, rbab057. [CrossRef]

57. Luo, R.; Li, F.; Wang, Y.; Zou, H.; Shang, J.; Fan, Y.; Liu, H.; Xu, Z.; Li, R.; Liu, H. MXene-modified 3D printed scaffold for photothermal therapy and facilitation of oral mucosal wound reconstruction. *Mater. Des.* **2023**, *227*, 111731. [CrossRef]

58. Fan, Y.; Li, F.; Zou, H.; Xu, Z.; Liu, H.; Luo, R.; Zhang, G.; Li, R.; Yan, Y.; Liu, H. Photothermal effect of indocyanine green modified scaffold inhibits oral squamous cell carcinoma and promotes wound healing. *Biomater. Adv.* **2022**, *137*, 212811. [CrossRef] [PubMed]

59. Mackey, M.A.; Ali, M.R.K.; Austin, L.A.; Near, R.D.; El-Sayed, M.A. The Most Effective Gold Nanorod Size for Plasmonic Photothermal Therapy: Theory and In Vitro Experiments. *J. Phys. Chem. B* **2014**, *118*, 1319–1326. [CrossRef]

60. Dickerson, E.B.; Dreaden, E.C.; Huang, X.; El-Sayed, I.H.; Chu, H.; Pushpanketh, S.; McDonald, J.F.; El-Sayed, M.A. Gold nanorod assisted near-infrared plasmonic photothermal therapy (PPTT) of squamous cell carcinoma in mice. *Cancer Lett.* **2008**, *269*, 57–66. [CrossRef]

61. Mehdizadeh, A.; Pandesh, S.; Shakeri-Zadeh, A.; Kamrava, S.K.; Habib-Agahi, M.; Farhadi, M.; Pishghadam, M.; Ahmadi, A.; Arami, S.; Fedutik, Y. The effects of folate-conjugated gold nanorods in combination with plasmonic photothermal therapy on mouth epidermal carcinoma cells. *Lasers Med. Sci.* **2013**, *29*, 939–948. [CrossRef] [PubMed]

62. Liao, Y.-T.; Liu, C.-H.; Chin, Y.; Chen, S.-Y.; Liu, S.H.; Hsu, Y.-C.; Wu, K.C.W. Biocompatible and multifunctional gold nanorods for effective photothermal therapy of oral squamous cell carcinoma. *J. Mater. Chem. B* **2019**, *7*, 4451–4460. [CrossRef]

63. Rao, L.; Bu, L.-L.; Ma, L.; Wang, W.; Liu, H.; Wan, D.; Liu, J.-F.; Li, A.; Guo, S.-S.; Zhang, L.; et al. Platelet-Facilitated Photothermal Therapy of Head and Neck Squamous Cell Carcinoma. *Angew. Chem. Int. Ed.* **2018**, *57*, 986–991. [CrossRef]

64. Huang, X.; El-Sayed, I.H.; Qian, W.; El-Sayed, M.A. Cancer Cell Imaging and Photothermal Therapy in the Near-Infrared Region by Using Gold Nanorods. *J. Am. Chem. Soc.* **2006**, *128*, 2115–2120. [CrossRef] [PubMed]

65. Afifi, M.M.; El Sheikh, S.M.; Abdelsalam, M.M.; Ramadan, H.; Omar, T.A.; El Tantawi, M.; Abdel-Razek, K.M.; Mohamed, M. Therapeutic efficacy of plasmonic photothermal nanoparticles in hamster buccal pouch carcinoma. *Oral Surg. Oral Med. Oral Pathol. Oral Radiol.* **2013**, *115*, 743–751. [CrossRef]

66. Elsayed, I.; Huang, X.; Elsayed, M. Selective laser photo-thermal therapy of epithelial carcinoma using anti-EGFR antibody conjugated gold nanoparticles. *Cancer Lett.* **2006**, *239*, 129–135. [CrossRef]

67. Chen, D.; Chen, Z.; Wang, Z.; Yang, Y.; Jiang, Y.; Hu, C. Photothermal effect of nano-copper sulfide against tongue squamous cell carcinoma. *J. South. Med. Univ.* **2021**, *41*, 1843–1849.

68. Su, J.; Lu, S.; Jiang, S.; Li, B.; Liu, B.; Sun, Q.; Li, J.; Wang, F.; Wei, Y. Engineered Protein Photo-Thermal Hydrogels for Outstanding In Situ Tongue Cancer Therapy. *Adv. Mater.* **2021**, *33*, 2100619. [CrossRef]

69. Fekrazad, R.; Hakimiha, N.; Farokhi, E.; Rasaee, M.J.; Ardestani, M.S.; Kalhori, K.A.; Sheikholeslami, F. Treatment of oral squamous cell carcinoma using anti-HER2 immunonanoshells. *Int. J. Nanomed.* **2011**, *6*, 2749–2755. [CrossRef]

70. Bu, L.-L.; Rao, L.; Yu, G.-T.; Chen, L.; Deng, W.-W.; Liu, J.-F.; Wu, H.; Meng, Q.-F.; Guo, S.-S.; Zhao, X.-Z.; et al. Cancer Stem Cell-Platelet Hybrid Membrane-Coated Magnetic Nanoparticles for Enhanced Photothermal Therapy of Head and Neck Squamous Cell Carcinoma. *Adv. Funct. Mater.* **2019**, *29*, 1807733. [CrossRef]

71. Wu, Q.; Chen, L.; Huang, X.; Lin, J.; Gao, J.; Yang, G.; Wu, Y.; Wang, C.; Kang, X.; Yao, Y.; et al. A biomimetic nanoplatform for customized photothermal therapy of HNSCC evaluated on patient-derived xenograft models. *Int. J. Oral Sci.* **2023**, *15*, 9. [CrossRef] [PubMed]

72. Li, Z.; Liu, Q.; Zhang, Y.; Yang, Y.; Zhou, X.; Peng, W.; Liang, Z.; Zeng, X.; Wang, Q.; Gao, N. Charge-reversal nanomedicine based on black phosphorus for the development of A Novel photothermal therapy of oral cancer. *Drug Deliv.* **2021**, *28*, 700–708. [CrossRef]

73. Das, R.K.; Panda, S.; Bhol, C.S.; Bhutia, S.K.; Mohapatra, S. N-Doped Carbon Quantum Dot (NCQD)-Deposited Carbon Capsules for Synergistic Fluorescence Imaging and Photothermal Therapy of Oral Cancer. *Langmuir* **2019**, *35*, 15320–15329. [CrossRef] [PubMed]

74. Pan, X.; Gao, A.; Hu, Y.; Hu, Z.; Xie, C.; Lin, Z. Gadolinium-containing semiconducting polymer nanoparticles for magnetic resonance/fluorescence dual-modal imaging and photothermal therapy of oral squamous cell carcinoma. *Nano Res.* **2023**, *16*, 2808–2820. [CrossRef]

75. Yang, Z.; Zhao, Y.; Li, Y.; Song, L.; Lin, Y.; Liu, K.; Zhang, Y.; Zvyagin, A.V.; Fang, L.; Sun, Y.; et al. Au/Mn nanodot platform for in vivo CT/MRI/FI multimodal bioimaging and photothermal therapy against tongue cancer. *J. Mater. Chem. B* **2023**, *11*, 4752–4762. [CrossRef] [PubMed]

76. Men, C.; Zhang, Y.; Shi, P.; Tang, Z.; Cheng, X. alphanubeta3 integrin-targeted ICG-derived probes for imaging-guided surgery and photothermal therapy of oral cancer. *Analyst* **2023**, *148*, 6334–6340. [CrossRef]

77. Zhang, L.; Chu, C.; Lin, X.; Sun, R.; Li, Z.; Chen, S.; Liu, Y.; Wu, J.; Yu, Z.; Liu, X. Tunable Nanoparticles with Aggregation-Induced Emission Heater for Precise Synergistic Photothermal and Thermodynamic Oral Cancer Therapy of Patient-Derived Tumor Xenograft. *Adv. Sci.* **2023**, *10*, 2205780. [CrossRef]

78. Wang, B.; Wang, J.-H.; Liu, Q.; Huang, H.; Chen, M.; Li, K.; Li, C.; Yu, X.-F.; Chu, P.K. Rose-bengal-conjugated gold nanorods for in vivo photodynamic and photothermal oral cancer therapies. *Biomaterials* **2014**, *35*, 1954–1966. [CrossRef]

79. Song, W.; Li, Y.; Wang, Y.; Wang, D.; He, D.; Chen, W.; Yin, W.; Yang, W. Indocyanine Green-Loaded Gold Nanoflowers@Two Layers of Silica Nanocomposites for Photothermal and Photodynamic Therapy of Oral Carcinoma. *J. Biomed. Nanotechnol.* **2017**, *13*, 1115–1123. [CrossRef]

80. Chu, C.-K.; Tu, Y.-C.; Hsiao, J.-H.; Yu, J.-H.; Yu, C.-K.; Chen, S.-Y.; Tseng, P.-H.; Chen, S.; Kiang, Y.-W.; Yang, C.C. Combination of photothermal and photodynamic inactivation of cancer cells through surface plasmon resonance of a gold nanoring. *Nanotechnology* **2016**, *27*, 115102. [CrossRef]

81. Bhana, S.; Lin, G.; Wang, L.; Starring, H.; Mishra, S.R.; Liu, G.; Huang, X. Near-Infrared-Absorbing Gold Nanopopcorns with Iron Oxide Cluster Core for Magnetically Amplified Photothermal and Photodynamic Cancer Therapy. *ACS Appl. Mater. Interfaces* **2015**, *7*, 11637–11647. [CrossRef] [PubMed]

82. Huang, X.; Deng, G.; Han, Y.; Yang, G.; Zou, R.; Zhang, Z.; Sun, S.; Hu, J. Right $Cu_{2-x}S$@MnS Core–Shell Nanoparticles as a Photo/$H_2O_2$-Responsive Platform for Effective Cancer Theranostics. *Adv. Sci.* **2019**, *6*, 1901461. [CrossRef] [PubMed]

83. Wang, G.; Zhang, F.; Tian, R.; Zhang, L.; Fu, G.; Yang, L.; Zhu, L. Nanotubes-Embedded Indocyanine Green–Hyaluronic Acid Nanoparticles for Photoacoustic-Imaging-Guided Phototherapy. *ACS Appl. Mater. Interfaces* **2016**, *8*, 5608–5617. [CrossRef]

84. Zheng, C.; Zhang, X.; Wang, L.; Zhou, X.; Yang, X.; Zhang, Z.; Huang, X. Versatile cobalt-glycerate nanoplatform for MR-guided neoadjuvant photo-therapy of oral squamous cell carcinoma. *Chem. Eng. J.* **2022**, *437*, 135476. [CrossRef]

85. Li, X.; Hao, M.; Liu, A.; Li, L.; Nešić, M.D.; Yang, B.; Liu, W.; Lin, Q. Dual-activity nanozyme as an oxygen pump to alleviate tumor hypoxia and enhance photodynamic/NIR-II photothermal therapy for sniping oral squamous cell carcinoma. *Acta Biomater.* **2024**, *190*, 476–487. [CrossRef]

86. Zhang, L.; Jing, D.; Wang, L.; Sun, Y.; Li, J.J.; Hill, B.; Yang, F.; Li, Y.; Lam, K.S. Unique Photochemo-Immuno-Nanoplatform against Orthotopic Xenograft Oral Cancer and Metastatic Syngeneic Breast Cancer. *Nano Lett.* **2018**, *18*, 7092–7103. [CrossRef]

87. Wu, Y.; Chen, F.; Huang, N.; Li, J.; Wu, C.; Tan, B.; Liu, Y.; Li, L.; Yang, C.; Shao, D.; et al. Near-infrared light-responsive hybrid hydrogels for the synergistic chemo-photothermal therapy of oral cancer. *Nanoscale* **2021**, *13*, 17168–17182. [CrossRef]

88. XIE, X.; SHAN, Y.; ZHANG, X.; WU, Y.; LIAO, J. Hyaluronic acid microneedles loaded with curcumin nanodrugs and new indocyanine green inhibits human tongue squamous carcinoma cells in vitro. *J. Zhejiang Univ. Med. Sci.* **2022**, *51*, 585–593. [CrossRef]

89.  Darwish, W.M.; Abdoon, A.S.; Shata, M.S.; Elmansy, M. Vincristine-loaded polymeric corona around gold nanorods for combination (chemo-photothermal) therapy of oral squamous carcinoma. *React. Funct. Polym.* **2020**, *151*, 104575. [CrossRef]

90.  El-Sherbiny, R.H.; Hassan, M.M.; El-Hossary, W.H.; Shata, M.S.; Darwish, W.M. Folate-targeted polymeric nanoparticles for efficient dual (chemo-photothermal) therapy of oral squamous carcinoma. *Int. J. Polym. Mater. Polym. Biomater.* **2020**, *70*, 414–424. [CrossRef]

91.  Mapanao, A.K.; Santi, M.; Voliani, V. Combined chemo-photothermal treatment of three-dimensional head and neck squamous cell carcinomas by gold nano-architectures. *J. Colloid Interface Sci.* **2021**, *582*, 1003–1011. [CrossRef]

92.  Liu, Z.; Shi, J.; Zhu, B.; Xu, Q. Development of a multifunctional gold nanoplatform for combined chemo-photothermal therapy against oral cancer. *Nanomedicine* **2020**, *15*, 661–676. [CrossRef]

93.  Li, R.; Liu, C.; Wan, C.; Liu, T.; Zhang, R.; Du, J.; Wang, X.; Jiao, X.; Gao, R.; Li, B. A Targeted and pH-Responsive Nano-Graphene Oxide Nanoparticle Loaded with Doxorubicin for Synergetic Chemo-Photothermal Therapy of Oral Squamous Cell Carcinoma. *Int. J. Nanomed.* **2023**, *18*, 3309–3324. [CrossRef] [PubMed]

94.  Li, R.; Wan, C.; Li, Y.; Jiao, X.; Liu, T.; Gu, Y.; Gao, R.; Liu, J.; Li, B. Nanocarrier-based drug delivery system with dual targeting and NIR/pH response for synergistic treatment of oral squamous cell carcinoma. *Colloids Surf. B-Biointerfaces* **2024**, *244*, 114179. [CrossRef] [PubMed]

95.  Li, R.; Li, Y.; Song, Z.; Gu, Y.; Jiao, X.; Wan, C.; Liu, T.; Zhang, R.; Gao, R.; Wang, X. A Graphene-Based Lipid Modulation Nanoplatform for Synergetic Lipid Starvation/Chemo/Photothermal Therapy of Oral Squamous Cell Carcinoma. *Int. J. Nanomed.* **2024**, *19*, 11235–11255. [CrossRef] [PubMed]

96.  Anup, N.; Gadeval, A.; Mule, S.R.; Gupta, T.; Tekade, R.K. Plasmonic laser-responsive BioDissolve 3D-printed graphene@cisplatin-implant for prevention of post-surgical relapse of oral cancer. *Int. J. Pharm.* **2024**, *657*, 124123. [CrossRef]

97.  Lin, M.; Wang, D.; Liu, S.; Huang, T.; Sun, B.; Cui, Y.; Zhang, D.; Sun, H.; Zhang, H.; Sun, H.; et al. Cupreous Complex-Loaded Chitosan Nanoparticles for Photothermal Therapy and Chemotherapy of Oral Epithelial Carcinoma. *ACS Appl. Mater. Interfaces* **2015**, *7*, 20801–20812. [CrossRef]

98.  Liu, S.; Wang, L.; Li, S.; Meng, X.; Sun, B.; Zhang, X.; Zhang, L.; Liu, Y.; Lin, M.; Zhang, H.; et al. Multidrug resistant tumors-aimed theranostics on the basis of strong electrostatic attraction between resistant cells and nanomaterials. *Biomater. Sci.* **2019**, *7*, 4990–5001. [CrossRef]

99.  Song, W.; Gong, J.; Wang, Y.; Zhang, Y.; Zhang, H.; Zhang, W.; Zhang, H.; Liu, X.; Zhang, T.; Yin, W.; et al. Gold nanoflowers with mesoporous silica as "nanocarriers" for drug release and photothermal therapy in the treatment of oral cancer using near-infrared (NIR) laser light. *J. Nanopart. Res.* **2016**, *18*, 101. [CrossRef]

100.  Xu, Y.; Hao, Y.; Li, W.; Xiao, Y.; Zhou, T.; Hu, D.; Liu, Q.; Zhou, X.; Qian, Z. Near-Infrared Responsive Doxorubicin Loaded Hollow Mesoporous Prussian Blue Nanoparticles Combined with Dissolvable Hyaluronic Acid Microneedle System for Human Oral Squamous Cell Carcinoma Therapy. *J. Biomed. Nanotechnol.* **2020**, *16*, 721–738. [CrossRef]

101.  Chen, J.; Li, Q.; Wang, F.; Yang, M.; Xie, L.; Zeng, X. Biosafety, Nontoxic Nanoparticles for VL–NIR Photothermal Therapy Against Oral Squamous Cell Carcinoma. *ACS Omega* **2021**, *6*, 11240–11247. [CrossRef] [PubMed]

102.  Jin, R.; Xie, J.; Yang, X.; Tian, Y.; Yuan, P.; Bai, Y.; Liu, S.; Cai, B.; Chen, X. A tumor-targeted nanoplatform with stimuli-responsive cascaded activities for multiple model tumor therapy. *Biomater. Sci.* **2020**, *8*, 1865–1874. [CrossRef] [PubMed]

103.  Neshastehriz, A.; Tabei, M.; Maleki, S.; Eynali, S.; Shakeri-Zadeh, A. Photothermal therapy using folate conjugated gold nanoparticles enhances the effects of 6 MV X-ray on mouth epidermal carcinoma cells. *J. Photochem. Photobiol. B Biol.* **2017**, *172*, 52–60. [CrossRef]

104.  Wang, B.-K.; Yu, X.-F.; Wang, J.-H.; Li, Z.-B.; Li, P.-H.; Wang, H.; Song, L.; Chu, P.K.; Li, C. Gold-nanorods-siRNA nanoplex for improved photothermal therapy by gene silencing. *Biomaterials* **2016**, *78*, 27–39. [CrossRef]

105.  Bu, L.-L.; Wang, H.-Q.; Pan, Y.; Chen, L.; Wu, H.; Wu, X.; Zhao, C.; Rao, L.; Liu, B.; Sun, Z.-J. Gelatinase-sensitive nanoparticles loaded with photosensitizer and STAT3 inhibitor for cancer photothermal therapy and immunotherapy. *J. Nanobiotechnol.* **2021**, *19*, 379. [CrossRef] [PubMed]

106.  Ran, J.; Liu, T.; Song, C.; Wei, Z.; Tang, C.; Cao, Z.; Zou, H.; Zhang, X.; Cai, Y.; Han, W. Rhythm Mild-Temperature Photothermal Therapy Enhancing Immunogenic Cell Death Response in Oral Squamous Cell Carcinoma. *Adv. Healthc. Mater.* **2022**, *12*, 2202360. [CrossRef]

107.  Qian, M.; Cheng, Z.; Luo, G.; Galluzzi, M.; Shen, Y.; Li, Z.; Yang, H.; Yu, X.F. Molybdenum Diphosphide Nanorods with Laser-Potentiated Peroxidase Catalytic/Mild-Photothermal Therapy of Oral Cancer. *Adv. Sci.* **2021**, *9*, 2101527. [CrossRef]

108.  Sun, H.; Wang, X.; Guo, Z.; Hu, Z.; Yin, Y.; Duan, S.; Jia, W.; Lu, W.; Hu, J. $Fe_3O_4$ Nanoparticles That Modulate the Polarisation of Tumor-Associated Macrophages Synergize with Photothermal Therapy and Immunotherapy (PD-1/PD-L1 Inhibitors) to Enhance Anti-Tumor Therapy. *Int. J. Nanomed.* **2024**, *19*, 7185–7200. [CrossRef]

109.  Bai, L.; Yang, M.; Wu, J.; You, R.; Chen, Q.; Cheng, Y.; Qian, Z.; Yang, X.; Wang, Y.; Liu, Y. An injectable adhesive hydrogel for photothermal ablation and antitumor immune activation against bacteria-associated oral squamous cell carcinoma. *Acta Biomater.* **2024**, *186*, 229–245. [CrossRef]

110.  Zeng, J.-j.; Tang, Z.-g.; Zou, J.; Yu, J.-g. Black phosphorous nanosheets–gold nanoparticles–cisplatin for photothermal/photodynamic treatment of oral squamous cell carcinoma. *Trans. Nonferrous Met. Soc. China* **2021**, *31*, 2812–2822. [CrossRef]

111. Wang, Y.; Xie, D.; Pan, J.; Xia, C.; Fan, L.; Pu, Y.; Zhang, Q.; Ni, Y.H.; Wang, J.; Hu, Q. A near infrared light-triggered human serum albumin drug delivery system with coordination bonding of indocyanine green and cisplatin for targeting photochemistry therapy against oral squamous cell cancer. *Biomater. Sci.* **2019**, *7*, 5270–5282. [CrossRef]

112. Wei, Z.; Zhang, H.; Zou, H.; Song, C.; Zhao, S.; Cao, Z.; Zhang, X.; Zhang, G.; Cai, Y.; Han, W. A novel second near-infrared theranostic agent: A win–win strategy of tracing and blocking tumor-associated vessels for oral squamous cell carcinoma. *Mater. Today Nano* **2022**, *17*, 100172. [CrossRef]

113. Xue, X.; Huang, Y.; Bo, R.; Jia, B.; Wu, H.; Yuan, Y.; Wang, Z.; Ma, Z.; Jing, D.; Xu, X.; et al. Trojan Horse nanotheranostics with dual transformability and multifunctionality for highly effective cancer treatment. *Nat. Commun.* **2018**, *9*, 3653. [CrossRef]

114. Shi, S.; Wang, Y.; Wang, B.; Chen, Q.; Wan, G.; Yang, X.; Zhang, J.; Zhang, L.; Li, C.; Wang, Y. Homologous-targeting biomimetic nanoparticles for photothermal therapy and Nrf2-siRNA amplified photodynamic therapy against oral tongue squamous cell carcinoma. *Chem. Eng. J.* **2020**, *388*, 124268. [CrossRef]

115. Song, C.; Zhang, X.; Cao, Z.; Wei, Z.; Zhou, M.; Wang, Y.; Han, S.; Cai, Y.; Han, W. Regulating tumor cholesterol microenvironment to enhance photoimmunotherapy in oral squamous cell carcinoma. *Chem. Eng. J.* **2023**, *462*, 142160. [CrossRef]

116. Chen, Q.; Shan, T.; Liang, Y.; Xu, Y.; Shi, E.; Wang, Y.; Li, C.; Wang, Y.; Cao, M. A biomimetic phototherapeutic nanoagent based on bacterial double-layered membrane vesicles for comprehensive treatment of oral squamous cell carcinoma. *J. Mater. Chem. B* **2023**, *11*, 11265–11279. [CrossRef] [PubMed]

117. Chen, L.; Yin, Q.; Zhang, H.; Zhang, J.; Yang, G.; Weng, L.; Liu, T.; Xu, C.; Xue, P.; Zhao, J.; et al. Protecting Against Postsurgery Oral Cancer Recurrence with an Implantable Hydrogel Vaccine for In Situ Photoimmunotherapy. *Adv. Sci.* **2024**, *11*, 2309053. [CrossRef] [PubMed]

118. Lin, L.; Song, C.; Wei, Z.; Zou, H.; Han, S.; Cao, Z.; Zhang, X.; Zhang, G.; Ran, J.; Cai, Y.; et al. Multifunctional photodynamic/photothermal nano-agents for the treatment of oral leukoplakia. *J. Nanobiotechnol.* **2022**, *20*, 106. [CrossRef]

119. Li, R.; Zhao, Y.; Liu, T.; Li, Y.; Wan, C.; Gao, R.; Liu, C.; Li, X.; Li, B. Nano-drug delivery system targeting FAP for the combined treatment of oral leukoplakia. *Drug Deliv. Transl. Res.* **2023**, *14*, 247–265. [CrossRef]

120. Zhu, T.; Sang, Z.; Ye, Z.; Guo, X.; Qu, X.; Hao, Y.; Wang, W. Local delivery of celecoxib/indocyanine green-loaded nanomodulators for combinational photothermal/photodynamic/anti-cyclooxygenase-2 therapy of oral leukoplakia. *Chem. Eng. J.* **2025**, *505*, 159734. [CrossRef]

121. Shrivastava, R.; Dube, A. Effect of the polyelectrolyte coating on the photothermal efficiency of gold nanorods and the photothermal induced cancer cell damage. *IET Nanobiotechnol.* **2017**, *11*, 909–916. [CrossRef] [PubMed]

122. Matsumoto, Y.; Nichols, J.W.; Toh, K.; Nomoto, T.; Cabral, H.; Miura, Y.; Christie, R.J.; Yamada, N.; Ogura, T.; Kano, M.R.; et al. Vascular bursts enhance permeability of tumour blood vessels and improve nanoparticle delivery. *Nat. Nanotechnol.* **2016**, *11*, 533–538. [CrossRef] [PubMed]

123. Bertrand, N.; Wu, J.; Xu, X.; Kamaly, N.; Farokhzad, O.C. Cancer nanotechnology: The impact of passive and active targeting in the era of modern cancer biology. *Adv. Drug Deliv. Rev.* **2014**, *66*, 2–25. [CrossRef]

124. Li, S.; Li, Y.; Shen, G.; Sun, J.; Abdelmohsen, L.K.E.A.; Yan, X.; van Hest, J.C.M. Flexible Morphological Regulation of Photothermal Nanodrugs: Understanding the Relationship between the Structure, Photothermal Effect, and Tumoral Biodistribution. *ACS Nano* **2025**, *19*, 2799–2808. [CrossRef] [PubMed]

125. Jacinto, C.; Silva, W.F.; Garcia, J.; Zaragosa, G.P.; Ilem, C.N.D.; Sales, T.O.; Santos, H.D.A.; Conde, B.I.C.; Barbosa, H.P.; Malik, S.; et al. Nanoparticles based image-guided thermal therapy and temperature feedback. *J. Mater. Chem. B* **2025**, *13*, 54–102. [CrossRef]

126. Xiao, Z.; Ji, C.; Shi, J.; Pridgen, E.M.; Frieder, J.; Wu, J.; Farokhzad, O.C. DNA self-assembly of targeted near-infrared-responsive gold nanoparticles for cancer thermo-chemotherapy. *Angew. Chem.-Int. Edit.* **2012**, *51*, 11853–11857. [CrossRef]

127. Ren, Y.; Yan, Y.; Qi, H. Photothermal conversion and transfer in photothermal therapy: From macroscale to nanoscale. *Adv. Colloid Interface Sci.* **2022**, *308*, 102753. [CrossRef]

128. Taheri-Ledari, R.; Ganjali, F.; Zarei-Shokat, S.; Dinmohammadi, R.; Asl, F.R.; Emami, A.; Mojtabapour, Z.S.; Rashvandi, Z.; Kashtiaray, A.; Jalali, F.; et al. Plasmonic porous micro- and nano-materials based on Au/Ag nanostructures developed for photothermal cancer therapy: Challenges in clinicalization. *Nanoscale Adv.* **2023**, *5*, 6768–6786. [CrossRef]

129. Nejabat, M.; Samie, A.; Ramezani, M.; Alibolandi, M.; Abnous, K.; Taghdisi, S.M. An Overview on Gold Nanorods as Versatile Nanoparticles in Cancer Therapy. *J. Control. Release* **2023**, *354*, 221–242. [CrossRef]

130. Alle, M.; Sharma, G.; Lee, S.-H.; Kim, J.-C. Next-generation engineered nanogold for multimodal cancer therapy and imaging: A clinical perspectives. *J. Nanobiotechnol.* **2022**, *20*, 222. [CrossRef]

131. Hu, M.; Chen, J.; Li, Z.-Y.; Au, L.; Hartland, G.V.; Li, X.; Marquez, M.; Xia, Y. Gold nanostructures: Engineering their plasmonic properties for biomedical applications. *Chem. Soc. Rev.* **2006**, *35*, 1084–1094. [CrossRef]

132. Shekhar, S.; Chauhan, M.; Sonali; Yadav, B.; Dutt, R.; Hu, L.; Muthu, M.S.; Singh, R.P. Enhanced Permeability and Retention Effect-Focused Tumor-Targeted Nanomedicines: Latest Trends, Obstacles and Future Perspective. *Nanomedicine* **2022**, *17*, 1213–1216. [CrossRef] [PubMed]

133. Danhier, F.; Feron, O.; Préat, V. To exploit the tumor microenvironment: Passive and active tumor targeting of nanocarriers for anti-cancer drug delivery. *J. Control. Release* **2010**, *148*, 135–146. [CrossRef] [PubMed]

134. Mansoori, G.A.; Brandenburg, K.S.; Shakeri-Zadeh, A. A comparative study of two folate-conjugated gold nanoparticles for cancer nanotechnology applications. *Cancers* **2010**, *2*, 1911–1928. [CrossRef]

135. Cai, L.; Wang, Y.; Peng, X.; Li, W.; Yuan, Y.; Tao, X.; Yao, X.; Lv, R. Gold Nanostars Combined with the Searched Antibody for Targeted Oral Squamous Cell Carcinoma Therapy. *ACS Biomater. Sci. Eng.* **2022**, *8*, 2664–2675. [CrossRef]

136. Ali, M.R.K.; Wu, Y.; Tang, Y.; Xiao, H.; Chen, K.; Han, T.; Fang, N.; Wu, R.; El-Sayed, M.A. Targeting cancer cell integrins using gold nanorods in photothermal therapy inhibits migration through affecting cytoskeletal proteins. *Proc. Natl. Acad. Sci. USA* **2017**, *114*, E5655–E5663. [CrossRef] [PubMed]

137. Sun, Q.; Wu, J.; Jin, L.; Hong, L.; Wang, F.; Mao, Z.; Wu, M. Cancer cell membrane-coated gold nanorods for photothermal therapy and radiotherapy on oral squamous cancer. *J. Mater. Chem. B* **2020**, *8*, 7253–7263. [CrossRef]

138. Ciftci, F.; Özarslan, A.C.; Kantarci, İ.C.; Yelkenci, A.; Tavukcuoglu, O.; Ghorbanpour, M. Advances in Drug Targeting, Drug Delivery, and Nanotechnology Applications: Therapeutic Significance in Cancer Treatment. *Pharmaceutics* **2025**, *17*, 121. [CrossRef]

139. Gao, Z.; Li, C.; Shen, J.; Ding, D. Organic optical agents for image-guided combined cancer therapy. *Biomed. Mater.* **2021**, *16*, 042009. [CrossRef]

140. Vyas, K.; Rathod, M.; Patel, M.M. Insight on nano drug delivery systems with targeted therapy in treatment of oral cancer. *Nanomed. Nanotechnol. Biol. Med.* **2023**, *49*, 102662. [CrossRef]

141. Jiang, J.; Hu, J.; Li, M.; Luo, M.; Dong, B.; Sitti, M.; Yan, X. NIR-II Fluorescent Thermophoretic Nanomotors for Superficial Tumor Photothermal Therapy. *Adv. Mater.* **2025**, *37*, 2417440. [CrossRef] [PubMed]

142. Mishra, R. Oral tumor heterogeneity, its implications for patient monitoring and designing anti-cancer strategies. *Pathol. Res. Pract.* **2024**, *253*, 154953. [CrossRef] [PubMed]

143. Overchuk, M.; Weersink, R.A.; Wilson, B.C.; Zheng, G. Photodynamic and Photothermal Therapies: Synergy Opportunities for Nanomedicine. *ACS Nano* **2023**, *17*, 7979–8003. [CrossRef] [PubMed]

144. Fan, W.; Yung, B.; Huang, P.; Chen, X. Nanotechnology for Multimodal Synergistic Cancer Therapy. *Chem. Rev.* **2017**, *117*, 13566–13638. [CrossRef]

145. Mou, J.; Lin, T.; Huang, F.; Chen, H.; Shi, J. Black titania-based theranostic nanoplatform for single NIR laser induced dual-modal imaging-guided PTT/PDT. *Biomaterials* **2016**, *84*, 13–24. [CrossRef]

146. Wei, G.; Wang, Y.; Yang, G.; Wang, Y.; Ju, R. Recent progress in nanomedicine for enhanced cancer chemotherapy. *Theranostics* **2021**, *11*, 6370–6392. [CrossRef]

147. Juthani, R.; Punatar, S.; Mittra, I. New light on chemotherapy toxicity and its prevention. *BJC Rep.* **2024**, *2*, 41. [CrossRef]

148. Aloss, K.; Hamar, P. Augmentation of the EPR effect by mild hyperthermia to improve nanoparticle delivery to the tumor. *Biochim. Biophys. Acta-Rev. Cancer* **2024**, *1879*, 189109. [CrossRef]

149. Gormley, A.J.; Larson, N.; Sadekar, S.; Robinson, R.; Ray, A.; Ghandehari, H. Guided Delivery of Polymer Therapeutics Using Plasmonic Photothermal Therapy. *Nano Today* **2012**, *7*, 158–167. [CrossRef]

150. Mendenhall, W.M.; Holtzman, A.L.; Dagan, R.; Bryant, C.M.; Hitchcock, K.E.; Amdur, R.J.; Fernandes, R.P. Current Role of Radiotherapy in the Management of Oral Cavity Squamous Cell Carcinoma. *Craniomaxillofacial Trauma Reconstr.* **2021**, *14*, 79–83. [CrossRef]

151. Pawlik, T.M.; Keyomarsi, K. Role of cell cycle in mediating sensitivity to radiotherapy. *Int. J. Radiat. Oncol. Biol. Phys.* **2004**, *59*, 928–942. [CrossRef]

152. Liu, J.; Yang, Y.; Zhu, W.; Yi, X.; Dong, Z.; Xu, X.; Chen, M.; Yang, K.; Lu, G.; Jiang, L.; et al. Nanoscale metal-organic frameworks for combined photodynamic & radiation therapy in cancer treatment. *Biomaterials* **2016**, *97*, 1–9. [PubMed]

153. Deng, Y.; Li, E.; Cheng, X.; Zhu, J.; Lu, S.; Ge, C.; Gu, H.; Pan, Y. Facile preparation of hybrid core-shell nanorods for photothermal and radiation combined therapy. *Nanoscale* **2016**, *8*, 3895–3899. [CrossRef]

154. Guo, S.; Yao, Y.; Tang, Y.; Xin, Z.; Wu, D.; Ni, C.; Huang, J.; Wei, Q.; Zhang, T. Radiation-induced tumor immune microenvironments and potential targets for combination therapy. *Signal Transduct. Target. Ther.* **2023**, *8*, 205. [CrossRef] [PubMed]

155. Bai, X.; Wang, Y.; Song, Z.; Feng, Y.; Chen, Y.; Zhang, D.; Lin, F. The Basic Properties of Gold Nanoparticles and their Applications in Tumor Diagnosis and Treatment. *Int. J. Mol. Sci.* **2020**, *21*, 2480. [CrossRef] [PubMed]

156. Her, S.; Jaffray, D.A.; Allen, C. Gold nanoparticles for applications in cancer radiotherapy: Mechanisms and recent advancements. *Adv. Drug Deliv. Rev.* **2017**, *109*, 84–101. [CrossRef]

157. Teo, P.Y.; Cheng, W.; Hedrick, J.L.; Yang, Y.Y. Co-delivery of drugs and plasmid DNA for cancer therapy. *Adv. Drug Deliv. Rev.* **2016**, *98*, 41–63. [CrossRef]

158. Tang, F.; Ding, A.; Xu, Y.; Ye, Y.; Li, L.; Xie, R.; Huang, W. Gene and Photothermal Combination Therapy: Principle, Materials, and Amplified Anticancer Intervention. *Small* **2024**, *20*, 2307078. [CrossRef]

159. Li, M.; Hou, M.; Wu, Q.; Jiang, Y.; Jia, G.; Wu, X.; Zhang, C. Simultaneous Inhibition of Heat Shock Response and Autophagy with Bimetallic Mesoporous Nanoparticles to Enhance Mild-Temperature Photothermal Therapy. *Small Struct.* **2023**, *4*, 2300132. [CrossRef]

160. Wang, S.; Tian, Y.; Tian, W.; Sun, J.; Zhao, S.; Liu, Y.; Wang, C.; Tang, Y.; Ma, X.; Teng, Z.; et al. Selectively Sensitizing Malignant Cells to Photothermal Therapy Using a CD44-Targeting Heat Shock Protein 72 Depletion Nanosystem. *ACS Nano* **2016**, *10*, 8578–8590. [CrossRef]

161. Chang, M.; Hou, Z.; Wang, M.; Li, C.; Lin, J. Recent Advances in Hyperthermia Therapy-Based Synergistic Immunotherapy. *Adv. Mater.* **2021**, *33*, 2004788. [CrossRef]

162. Ribas, A.; Wolchok, J.D. Cancer immunotherapy using checkpoint blockade. *Science* **2018**, *359*, 1350–1355. [CrossRef]

163. June, C.H.; O'Connor, R.S.; Kawalekar, O.U.; Ghassemi, S.; Milone, M.C. CAR T cell immunotherapy for human cancer. *Science* **2018**, *359*, 1361–1365. [CrossRef]

164. Goyal, P.M.; Kumar, M.; Kiran, M.; Srivastava, S.; Roy, S.K.; Garg, S.; Salunke, S.; Lader, S.; Quadri, K.; Ansari, A.; et al. Optimizing surgical margins in oral cancer without frozen section: A single center retrospective study. *Eur. J. Surg. Oncol.* **2025**, *51*, 109360. [CrossRef]

165. Baddour, H.M., Jr.; Magliocca, K.R.; Chen, A.Y. The importance of margins in head and neck cancer. *J. Surg. Oncol.* **2016**, *113*, 248–255. [CrossRef]

166. Zanoni, D.K.; Migliacci, J.C.; Xu, B.; Katabi, N.; Montero, P.H.; Ganly, I.; Shah, J.P.; Wong, R.J.; Ghossein, R.A.; Patel, S.G. A Proposal to Redefine Close Surgical Margins in Squamous Cell Carcinoma of the Oral Tongue. *JAMA Otolaryngol. Head Neck Surg.* **2017**, *143*, 555–560. [CrossRef]

167. Smits, R.W.H.; Koljenović, S.; Hardillo, J.A.; Hove, I.T.; Meeuwis, C.A.; Sewnaik, A.; Dronkers, E.A.; Schut, T.C.B.; Langeveld, T.P.M.; Molenaar, J.; et al. Resection margins in oral cancer surgery: Room for improvement. *Head Neck-J. Sci. Spec. Head Neck* **2016**, *38* (Suppl. S1), E2197–E2203.

168. Hainfeld, J.F.; Dilmanian, F.A.; Slatkin, D.N.; Smilowitz, H.M. Radiotherapy enhancement with gold nanoparticles. *J. Pharm. Pharmacol.* **2008**, *60*, 977–985. [CrossRef]

169. Wang, X.; Zhang, J.; Wang, Y.; Wang, C.; Xiao, J.; Zhang, Q.; Cheng, Y. Multi-responsive photothermal-chemotherapy with drug-loaded melanin-like nanoparticles for synergetic tumor ablation. *Biomaterials* **2016**, *81*, 114–124. [CrossRef]

170. Yokoi, A.; Maruyama, T.; Yamanaka, R.; Takeuchi, N.; Morita, M.; Ekuni, D. Relationship among cancer treatment, quality of life, and oral function in head and neck cancer survivors: A cross-sectional study. *Support. Care Cancer* **2024**, *32*, 809. [CrossRef]

171. Yuwanati, M.; Gondivkar, S.; Sarode, S.C.; Gadbail, A.; Desai, A.; Mhaske, S.; Pathak, S.K.; N Khatib, M. Oral Health-Related Quality of Life in Oral Cancer Patients: Systematic Review and Meta-Analysis. *Future Oncol.* **2021**, *17*, 979–990. [CrossRef]

172. Zanoni, D.K.; Montero, P.H.; Migliacci, J.C.; Shah, J.P.; Wong, R.J.; Ganly, I.; Patel, S.G. Survival outcomes after treatment of cancer of the oral cavity (1985–2015). *Oral Oncol.* **2019**, *90*, 115–121. [CrossRef]

173. Cortina, L.E.; Moverman, D.J.; Zhao, Y.; Goss, D.; Zenga, J.; Puram, S.V.; Varvares, M.A. Functional considerations between flap and non-flap reconstruction in oral tongue cancer: A systematic review. *Oral Oncol.* **2023**, *147*, 106596. [CrossRef]

174. Al-Aroomi, M.A.; Al-Worafi, N.A.; Ma, Y.; Alkebsi, K.; Mohamed, A.A.S.; Jiang, C. Patient-reported outcomes after oral cancer reconstructions with radial and ulnar forearm-free flaps. *Oral Dis.* **2024**, *30*, 4878–4885. [CrossRef]

175. Accorona, R.; Di Furia, D.; Cremasco, A.; Gazzini, L.; Mevio, N.; Pilolli, F.; Achena, A.; Iftikhar, H.; Awny, S.; Ormellese, G.L.; et al. Oral Reconstruction with Locoregional Flaps after Cancer Ablation: A Systematic Review of the Literature. *J. Clin. Med.* **2024**, *13*, 4181. [CrossRef]

176. Nie, R.; Sun, Y.; Lv, H.; Lu, M.; Huangfu, H.; Li, Y.; Zhang, Y.; Wang, D.; Wang, L.; Zhou, Y. 3D printing of MXene composite hydrogel scaffolds for photothermal antibacterial activity and bone regeneration in infected bone defect models. *Nanoscale* **2022**, *14*, 8112–8129. [CrossRef]

177. Wang, X.; Qian, Y.; Wang, S.; Wang, M.; Sun, K.; Cheng, Z.; Shao, Y.; Zhang, S.; Tang, C.; Chu, C.; et al. Accumulative Rolling Mg/PLLA Composite Membrane with Lamellar Heterostructure for Enhanced Bacteria Inhibition and Rapid Bone Regeneration. *Small* **2023**, *19*, 2301638. [CrossRef]

178. Wu, Y.; Zhang, X.; Tan, B.; Shan, Y.; Zhao, X.; Liao, J. Near-infrared light control of GelMA/PMMA/PDA hydrogel with mild photothermal therapy for skull regeneration. *Biomater. Adv.* **2022**, *133*, 112641. [CrossRef]

179. Liu, W.-S.; Chen, Z.; Lu, Z.-M.; Dong, J.-H.; Wu, J.-H.; Gao, J.; Deng, D.; Li, M. Multifunctional hydrogels based on photothermal therapy: A prospective platform for the postoperative management of melanoma. *J. Control. Release* **2024**, *371*, 406–428. [CrossRef]

180. Yu, Z.; Wang, H.; Ying, B.; Mei, X.; Zeng, D.; Liu, S.; Qu, W.; Pan, X.; Pu, S.; Li, R.; et al. Mild photothermal therapy assist in promoting bone repair: Related mechanism and materials. *Mater. Today Bio* **2023**, *23*, 100834. [CrossRef]

181. Zhu, H.; Qian, C.; Xiao, W.; Zhang, Q.; Ge, Z. Performance of a porous composite scaffold containing silk fibroin: Applied research repair on oral jaw epithelial defects. *Mater. Express* **2020**, *10*, 490–502. [CrossRef]

182. Gupta, P.; Adhikary, M.; Moses, J.C.; Kumar, M.; Bhardwaj, N.; Mandal, B.B. Biomimetic, Osteoconductive Non-mulberry Silk Fiber Reinforced Tricomposite Scaffolds for Bone Tissue Engineering. *ACS Appl. Mater. Interfaces* **2016**, *8*, 30797–30810. [CrossRef]

183. Suzuki, A.; Kodama, Y.; Miwa, K.; Kishimoto, K.; Hoshikawa, E.; Haga, K.; Sato, T.; Mizuno, J.; Izumi, K. Manufacturing micropatterned collagen scaffolds with chemical-crosslinking for development of biomimetic tissue-engineered oral mucosa. *Sci. Rep.* **2020**, *10*, 22192. [CrossRef] [PubMed]

184. Wang, X.; Mu, M.; Yan, J.; Han, B.; Ye, R.; Guo, G. 3D printing materials and 3D printed surgical devices in oral and maxillofacial surgery: Design, workflow and effectiveness. *Regen. Biomater.* **2024**, *11*, rbae066. [CrossRef] [PubMed]

185. Melke, J.; Midha, S.; Ghosh, S.; Ito, K.; Hofmann, S. Silk fibroin as biomaterial for bone tissue engineering. *Acta Biomater.* **2016**, *31*, 1–16. [CrossRef] [PubMed]

186. Milan, E.P.; Martins, V.C.A.; Horn, M.M.; Plepis, A.M.G. Influence of blend ratio and mangosteen extract in chitosan/collagen gels and scaffolds: Rheological and release studies. *Carbohydr Polym* **2022**, *292*, 119647. [CrossRef]

187. Loo, S.C.; Moore, T.; Banik, B.; Alexis, F. Biomedical applications of hydroxyapatite nanoparticles. *Curr. Pharm. Biotechnol.* **2010**, *11*, 333–342. [CrossRef]

188. Dai, W.; Zheng, Y.; Li, B.; Yang, F.; Chen, W.; Li, Y.; Deng, Y.; Bai, D.; Shu, R. A 3D-printed orthopedic implant with dual-effect synergy based on $MoS_2$ and hydroxyapatite nanoparticles for tumor therapy and bone regeneration. *Colloids Surf. B-Biointerfaces* **2023**, *228*, 113384. [CrossRef]

189. Knight, M.N.; Hankenson, K.D. Mesenchymal Stem Cells in Bone Regeneration. *Adv. Wound Care* **2013**, *2*, 306–316. [CrossRef]

190. Naara, S.; Andrews, C.; Sikora, A.; Williams, M.; Chambers, M.; Myers, J.; Amit, M. Oral Pre-malignancy: An Update on Novel Therapeutic Approaches. *Curr. Oncol. Rep.* **2024**, *26*, 1047–1056. [CrossRef]

191. van der Waal, I. Historical perspective and nomenclature of potentially malignant or potentially premalignant oral epithelial lesions with emphasis on leukoplakia-some suggestions for modifications. *Oral Surg. Oral Med. Oral Pathol. Oral Radiol.* **2018**, *125*, 577–581. [CrossRef]

192. Johnson, D.E.; Burtness, B.; Leemans, C.R.; Lui, V.W.Y.; Bauman, J.E.; Grandis, J.R. Head and neck squamous cell carcinoma. *Nat. Rev. Dis. Primers* **2020**, *6*, 92. [CrossRef] [PubMed]

193. Pimenta-Barros, L.A.; Ramos-García, P.; González-Moles, M.Á.; Aguirre-Urizar, J.M.; Warnakulasuriya, S. Malignant transformation of oral leukoplakia: Systematic review and comprehensive meta-analysis. *Oral Dis.* **2025**, *31*, 69–80. [CrossRef] [PubMed]